

Review

Biocompatible Iron Oxide Nanoparticles for Targeted Cancer Gene Therapy: A Review

Jinsong Zhang ¹, Tianyuan Zhang ^{1,*} and Jianqing Gao ^{1,2,*}¹ College of Pharmaceutical Sciences, Zhejiang University, Hangzhou 310058, China² Department of Pharmacy, the Second Affiliated Hospital, School of Medicine, Zhejiang University, Hangzhou 310058, China

* Correspondence: tianyuanzhang@zju.edu.cn (T.Z.); gaojianqing@zju.edu.cn (J.G.)

Abstract: In recent years, gene therapy has made remarkable achievements in tumor treatment. In a successfully cancer gene therapy, a smart gene delivery system is necessary for both protecting the therapeutic genes in circulation and enabling high gene expression in tumor sites. Magnetic iron oxide nanoparticles (IONPs) have demonstrated their bright promise for highly efficient gene delivery target to tumor tissues, partly due to their good biocompatibility, magnetic responsiveness, and extensive functional surface modification. In this review, the latest progress in targeting cancer gene therapy is introduced, and the unique properties of IONPs contributing to the efficient delivery of therapeutic genes are summarized with detailed examples. Furthermore, the diagnosis potentials and synergistic tumor treatment capacity of IONPs are highlighted. In addition, aiming at potential risks during the gene delivery process, several strategies to improve the efficiency or reduce the potential risks of using IONPs for cancer gene therapy are introduced and addressed. The strategies and applications summarized in this review provide a general understanding for the potential applications of IONPs in cancer gene therapy.

Keywords: iron oxide nanoparticles; gene delivery; tumor targeting; cancer treatment; tumor diagnosis



Citation: Zhang, J.; Zhang, T.; Gao, J. Biocompatible Iron Oxide

Nanoparticles for Targeted Cancer Gene Therapy: A Review.

Nanomaterials **2022**, *12*, 3323. <https://doi.org/10.3390/nano12193323>

Academic Editor: Jose Luis Arias Mediano

Received: 17 August 2022

Accepted: 20 September 2022

Published: 24 September 2022

Publisher's Note: MDPI stays neutral with regard to jurisdictional claims in published maps and institutional affiliations.



Copyright: © 2022 by the authors. Licensee MDPI, Basel, Switzerland. This article is an open access article distributed under the terms and conditions of the Creative Commons Attribution (CC BY) license (<https://creativecommons.org/licenses/by/4.0/>).

1. Introduction

Cancer is one of the most significant global threats to human life and health. Surgery, chemotherapy, and radiation therapy are the mainstays of clinical tumor treatment. However, the complexity of tumors and their microenvironment imposes limitations on the therapeutic efficiency using conventional treatment strategies. In addition, chemotherapy and radiation therapy may kill both tumor cells and normal cells due to their lack of specificity, resulting in several adverse side effects [1,2]. As a novel cancer treatment method, gene therapy can effectively inhibit tumor proliferation and growth by directly regulating key genes or proteins (e.g., KRAS, cMYC, MDR1, and PTEN), demonstrating attractive therapeutic effects in treating a variety of cancers, including lung, liver, breast, brain, and gastrointestinal tumors [2–4]. Notably, tumor suppression can be achieved in some gene therapy cases by modulating the tumor cell microenvironment by targeting tumor-associated angiogenesis, fibroblasts, and immune responses [5].

DNAs, small interfering RNAs (siRNAs), microRNAs (miRNAs), and messenger RNAs (mRNAs) are the most frequently used nucleic acid drugs for gene therapy [6–10]. In the cytoplasm, siRNA-induced silencing complexes are capable of particular complementary binding to target mRNA selectively and subsequent silencing of cancer-related genes. miRNAs can bind to particular mRNAs to inhibit their translation or promote degradation [11]. Unlike other pathways, DNA mainly enters the nucleus, where it regulates the expressions of target proteins through further transcription and translation [12]. Moreover, gene-editing technology provides more opportunities for cancer gene therapy. Using CRISPR/Cas9, an efficient gene-editing system consisting of single-guide RNA and Cas9

protein, target genes in tumors can be deleted, inserted, or modified to produce significant antitumor therapeutic effects [13,14].

Safe, effective, and programmable vectors are crucial to the success of gene therapy [15,16]. Direct delivery of naked gene drugs is susceptible to attack by various nucleases, resulting in less accumulation of gene drugs at the tumor sites [17]. Because of their considerable molecular weight, negative charges, and hydrophilicity, naked genes also have difficulty in entering cancer cells [18,19]. In vivo, naked genes are easily recognized and destroyed by extracellular and intracellular endonucleases, exonucleases, and the innate immune system [20–22]. Meanwhile, due to the inability of tumor-targeting, naked gene drugs may affect normal cells and tissues, thereby posing safety risks [23,24]. Consequently, selecting an appropriate gene delivery vehicle is necessary for successful cancer gene therapy.

2. IONPs for Gene Delivery Target to Cancer Cells

Currently, viral vectors, such as adenovirus, retrovirus, vaccinia virus, and herpes virus, are the most applied vectors for gene delivery, and more than 60% of clinical treatment trials employ viral vectors [18,25]. Viral vectors have been used to deliver therapeutic genes to cancer cells, and four viral–vector–based gene therapies have been clinically approved, including Talimogene laherparepvec, Mx–dnG1, H101, and Ad–p53 [26]. An important challenge in the current clinical trials of viral–vector–based gene therapy is the safety hazard from the innate or adaptive immune response caused by viral vectors. In addition, high production costs may be encountered when using viral vectors for large–scale production, limiting the clinical translation for gene delivery [27–30].

Using non–viral agents, such as polymers, liposomes, and micelles, to facilitate gene entry into tumor cells has garnered considerable attention [31,32]. Liposomes and nanoparticles are the most extensively researched non–viral carriers, showing major advantages to improve gene delivery efficiency, but are facing challenges of their short half–life, low biological activity, and potential hepatotoxicity [33,34]. In addition to liposomes, polyplex micelles encapsulating genetic drugs have been actively studied in cancer therapy, using anti–angiogenic [35–37] and suicide gene delivery [38–40]. However, limited blood circulation half–life due to liver sinusoidal capture remains the major critical hurdle [41,42]. Inorganic nanomaterials, such as gold, silver, and silicon dioxide, are recently developed for efficient gene delivery, showing advantages of controllable size and good uniformity [43]. However, it should be noted that these inorganic nanocarriers tend to accumulate in the liver [44] and kidney, resulting in potential toxicity, which limits their use as gene delivery vehicles [45–47].

Magnetic IONPs have more potential for tumor–targeted gene delivery than other inorganic nanomaterials due to their exceptional properties. These properties include superior magnetic responsiveness, simple preparation, ease of chemical functionalization, low toxicity, and high biocompatibility [48–51]. Luo et al. applied amino–ester lipid–modified superparamagnetic iron oxide nanoparticles (SPIONs) to deliver mRNA, showing advantages in a high mRNA–mediated protein expression and an increased r_2 relaxivity for magnetic resonance imaging (MRI). Hence, they thought IONPs had promising potential as delivery vehicles of mRNA for theranostic applications [9]. Research from Wang et al. demonstrated that IONPs coated with chitosan–polyethylene (PEG) had the ability to deliver siRNA to hepatocellular carcinoma in vitro and suppressed Luc expression. In a xenograft mouse model, the nanovector could specifically bind to tumors and induce remarkable inhibition of Luc expression [52].

Through electrostatic adsorption, surface–modified IONPs are loaded with large quantities of negative–charged genetic drugs. The therapeutic genes carried by IONPs can then be delivered to tumor cells under the navigation of an external magnetic field (Figure 1). IONPs have demonstrated their promising ability for targeting gene delivery to different types of tumors, such as breast cancer, glioma, cervical cancer, prostate cancer,

and gastric cancer (Table 1). Thus far, lots of studies have indicated the potent promise of IONPs in the treatment of solid tumors.

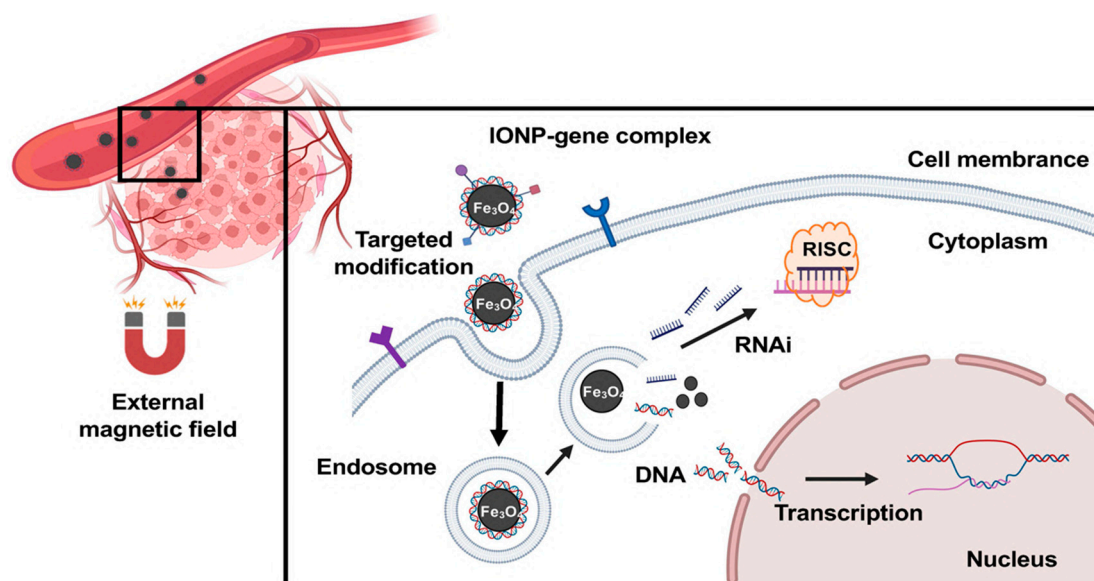


Figure 1. Schematic illustration of using IONPs to deliver gene drugs to tumor sites.

Table 1. Examples of using IONPs for efficient gene delivery targeting to tumors.

Coating Materials	Size	Payload	Tumor Models	Efficiency	References
Chitosan, PEI (MW 3.9 kDA)	54.23 nm (core: 31.33 nm)	pDsRed-MAX-N1	4T1 breast cancer cells in vitro	High transfection efficiency	[53]
Chitosan, PEI, PEG	184 ± 6 nm (core: around 150 nm)	pEGFP-CS2	Xenografted tumor of C6 glioma	45.2 ± 3.4% transfected	[54]
Folic acid, lipo-polymersomes	220–260 nm (core: 170–220 nm)	pDNA	Xenografted tumor of Hela cervical cancer	High cellular uptake rate; high transfection efficiency	[55]
Fluorinated PEG-PEI	93.29 ± 7.31 nm	siRNA	4T1 breast cancer cells in vitro	More than 90% transfected	[56]
PEI	around 26.12 nm (core: around 7.95 nm)	siRNA	Ca9-22 oral cancer cells in vitro	BCL-2 mRNA level reduced to 18%	[57]
Calcium phosphate, PEG	67 ± 17 nm (core: 16 ± 3 nm)	siRNA	MDA-MB 231 breast cancer cells in vitro	VEGF mRNA level reduced to around 60%	[58]
PEG, PEI	79.2 ± 0.68 nm	siRNA	PC3 prostate cancer cells in vitro	Prostate cancer cell viability significantly decreased	[59]
Folic-acid-functionalized PEI	around 120 nm	siRNA	SGC-7901 gastric cancer cells in vitro	PD-L1 mRNA level reduced by 90.93 ± 0.79%	[60]
Tumor-targeting peptide, dextran	20–30 nm (core: around 20 nm)	miRNA-10b	MDA-MB-231 breast cancer cells in vitro	10b miRNA level reduced by 74%	[61]

For example, Zhang et al. recently showed that IONPs could deliver siRNA to intracranial xenografted glioma and effectively reduced glutathione peroxidase 4 expression, resulting in a significantly improved inhibition of tumor growth [62]. Yang et al. found that using galactose- and polyetherimide-modified IONPs could largely enhance siRNA accumulation in orthotopic solid tumors for as long as 24 h after intravenous injection, resulting in a significant reduction in the volume of hepatocellular carcinoma, as well as liver/body weight ratio [63]. Moreover, Dan et al. recently demonstrated the promising potential of galactose (Gal)- and -polyethyleneimine (PEI)-coated SPIONs (Gal-PEI-SPIONs) for gene delivery and MRI in an in situ hepatic tumor model. The Gal-PEI-SPIONs showed the ability to selectively deliver siRNA-encoding telomerase reverse transcriptase genes to tumor sites in the liver after systemic injection, thereby showing a significant inhibition of tumor growth [64]. In addition, IONPs have also demonstrated the ability to inhibit tumor metastasis in animal models [65–67]. For example, after intravenous injection in the early stage of metastasis development, IONPs modified with the tumor-penetrating

peptide iRGD could target and reduce tumor growth in the brain [66]. Zhang et al. applied IONPs modified with 3-aminopropyltriethoxysilane for tumor-targeted delivery of cytosine-phosphate-guanine (CpG), a novel toll-like receptor 9 (TLR9) agonist, showing a good therapeutic effect to inhibit metastasis in 4T1 breast cancer [67].

The enhanced permeability and retention (EPR) effect is the ability of nanoparticles between 10 and 100 nm to passively penetrate the tumor site's complex and dense microvascular structure and persist in the tumor tissue for an extended period without being cleared by the lymphatic system [68]. The size of the nanoparticles plays an important role in the EPR effect of the nanocarriers [69]. Advantages of the controllable size of IONPs enable a better utilization of the EPR effect can be realized to deliver genetic drugs carrying nanoparticles targeting tumor sites. Different from the nonspecific mechanisms based on the EPR effect, the active targeting mechanisms approaching peptides, antibodies, and small molecules also play an important role in tumor targeting. Due to the exceptional surface functionalization capacity of IONPs, modified IONPs can bind to specific receptors on tumor cells, thereby facilitating the active targeting of IONP gene complexes to tumor sites [55,70,71]. In addition, the magnetic targeting of IONPs using gradient magnetic field gradient is crucial to drive IONPs actively target to the tumor tissue [72,73]. The properties of the magnetic field closely relate to the efficiency of magnetic targeting [74]. An external and static magnetic field between 0.2 and 0.6 T was reported to guide IONPs toward the tumor region [75]. The strength and location of the external magnetic field influence the magnetic response of IONPs, further affecting the efficiency of tumor-targeted gene delivery [50,65]. Solid tumors with a certain shape and position may facilitate the setting of an external magnetic field, thereby improving the magnetic targeting of nanoparticles to tumor sites and the accumulation of genetic drugs.

3. IONPs for Tumor Diagnosis and Combination Therapy

It has been reported that IONPs have functional advantages in cancer treatment, including magnetic resonance imaging, photothermal, photodynamic, magnetocaloric, and immune activation [76–78]. Combinations of gene therapy with imaging, chemotherapy drug delivery, enhanced immune response, radiotherapy, and phototherapy based on IONPs can be used to diagnose and treat tumors in a synergistic treatment (Figure 2).

3.1. IONPs for Tumor Cell Selected Imaging

By influencing transverse relaxation (T₂), magnetic IONPs with a size of less than 30 nm, are capable of being controlled by electromagnetic fields (EMFs) and used as contrast agents in MRI systems [79–81]. For example, due to the coupled spins of 3 d electrons unpaired with the cubic lattice of Fe³⁺ and Fe⁴⁺ cations, SPIONs can flip the orientation of their core protons when exposed to electromagnetic fields. This results in local field inhomogeneities and negative contrast in T₂-weighted imaging, which enables tissue imaging with high contrast and spatial resolution in MRI systems [82].

The imaging capabilities of IONPs confer significant advantages over other gene delivery vehicles, such as providing accurate diagnostic information for tumor lesion localization, which is crucial for precise and targeted therapy. MRI technology allows the observation of the biological distribution and pharmacokinetic properties of IONPs carrying gene drugs in various organ systems, indicating the gene delivery efficiency to the tumor site [83–85]. Mahajan et al. designed a siPLK1-conjugated streptavidin-conjugated dextran-coated SPION (siPLK1-StAv-SPION) delivery platform through directly knocking down cell-cycle-specific serine-threonine-kinase. This platform inhibited tumor cell apoptosis and proliferation by tumor-specific silencing of PLK1 and allowed for the non-invasive assessment of in vivo delivery efficiency by imaging tumor response (Figure 3) [86].

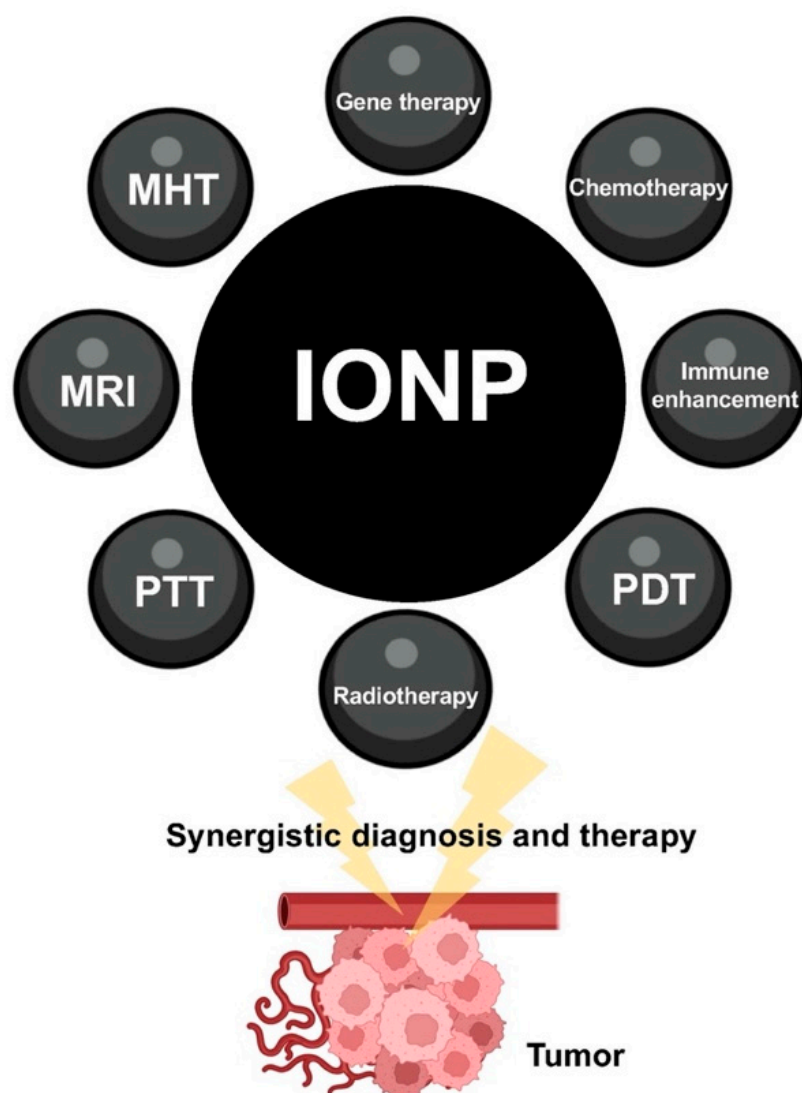


Figure 2. Gene therapy combining with other strategies to synergistically play a role in the diagnosis and treatment of tumors based on the versatility of IONPs.

3.2. IONPs for Co-Delivery of Therapeutic Genes and Chemotherapeutic Drugs

Chemotherapy drugs widely used in clinics today, such as cisplatin, paclitaxel, and doxorubicin (DOX), have a good killing effect on cancer cells but can also damage normal cells and tissues and cause noticeable side effects [87]. In recent years, the strategy of utilizing IONPs for the combined delivery of gene drugs and chemotherapeutic drugs has been demonstrated to be both feasible and highly effective [88–91]. Li et al. used PEG–PEI–coated IONPs to deliver microRNA–21 antisense oligonucleotide (ASO–miR–21) and gemcitabine (Gem) to pancreatic cancer cells. They observed that this co-delivery strategy effectively inhibited the growth and metastasis of tumor cells via the upregulation of tumor suppressor genes PDCD4 and PTEN and the inhibition of epithelial–mesenchymal transition [92]. Co-loading gene and chemical drugs on surface–modified IONPs not only enhances the killing effect on tumor cells via various mechanisms and pathways but also prevents damage from drugs to normal cells or tissues.

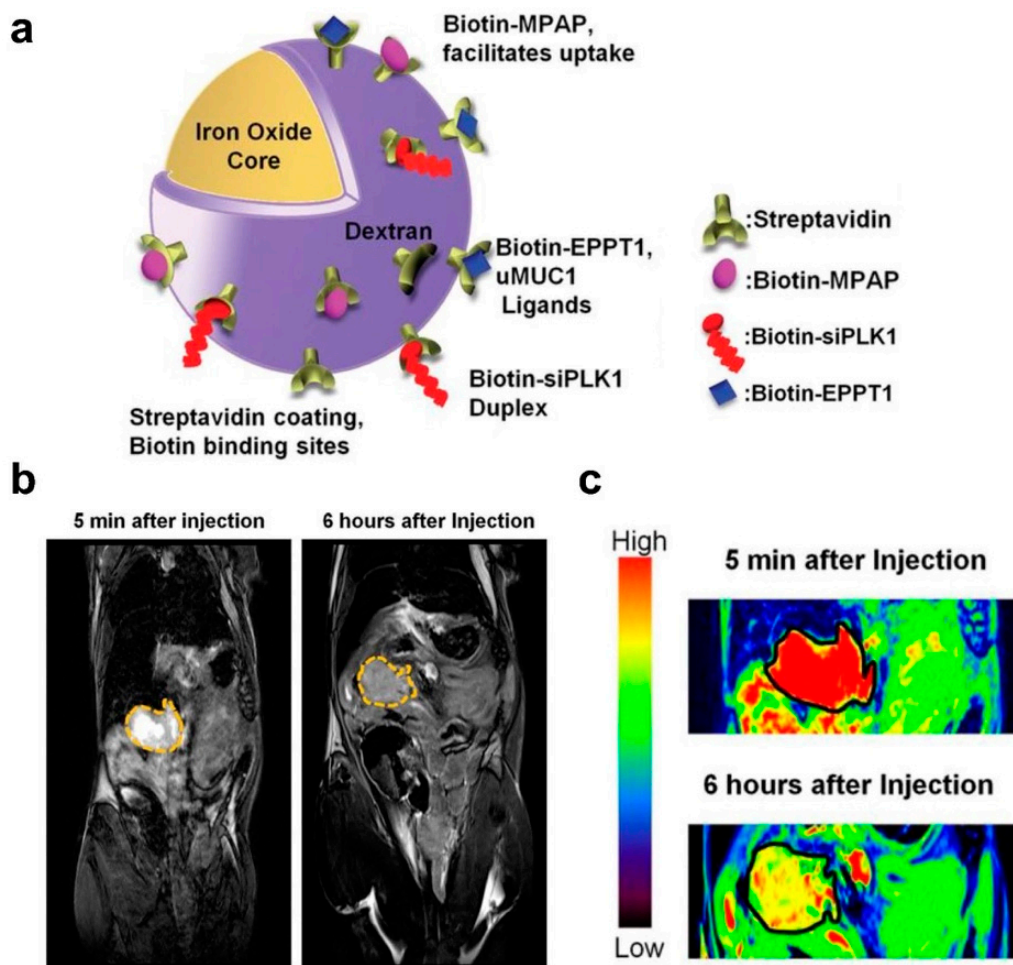


Figure 3. IONPs for gene delivery and in vivo tumor imaging. (a) Schematic representation of siPLK1–StAv–SPIONs. (b) In vivo MRI of mice bearing syngeneic orthotopic tumors was performed before and 6 h after intravenous injection of siPLK1–StAv–SPIONs. The dashed line marks the periphery of the tumor. (c) Color contrast images show decreased T2 relaxivity compared to pre-injection. Reprinted with permission from Ref. [86]. Copyright 2016, BMJ Publishing Group Ltd. and British Society of Gastroenterology.

3.3. IONPs for Inducing Antitumor Immune Response

The immune response can be often triggered after exogenous gene–drug–carrying IONPs are introduced into the body. Recent studies have shown that this immune activation induces the synergistic immune response to recognize and kill tumors, although this immune response is reduced in most drug delivery vehicle designs [93,94]. When exogenous genes are endocytosed, toll–like receptors in the immune system are activated, recognizing the genetic drugs and activating the type I interferon signaling pathway, which can activate various immune responses. Immune cells such as macrophages, T lymphocytes, B lymphocytes, and dendritic cells can be combined with chemotherapy drugs to kill tumor cells [95,96].

In a recent study, Meng et al. co–delivered peptide antigens and adjuvants (cytosine 5′ to a guanine dinucleotide repeat; CpG DNA) to dendritic cells (DCs) in the cytosol and lysosomes via membrane fusion and endocytosis with lipid–coated iron oxide nanoparticles (IONP–C/O@LPs), synergistically activating immature DCs. In addition, IONPs appeared to promote DC maturation by generating intracellular reactive oxygen species

during this process. Through subcutaneous injection, IONP–C/O@LPs accumulated in draining lymph nodes activated immature DCs efficiently and increased antigen–specific T cells in tumors and the spleen, inducing local and systemic antitumor immune responses and inhibiting tumor growth (Figure 4) [97].

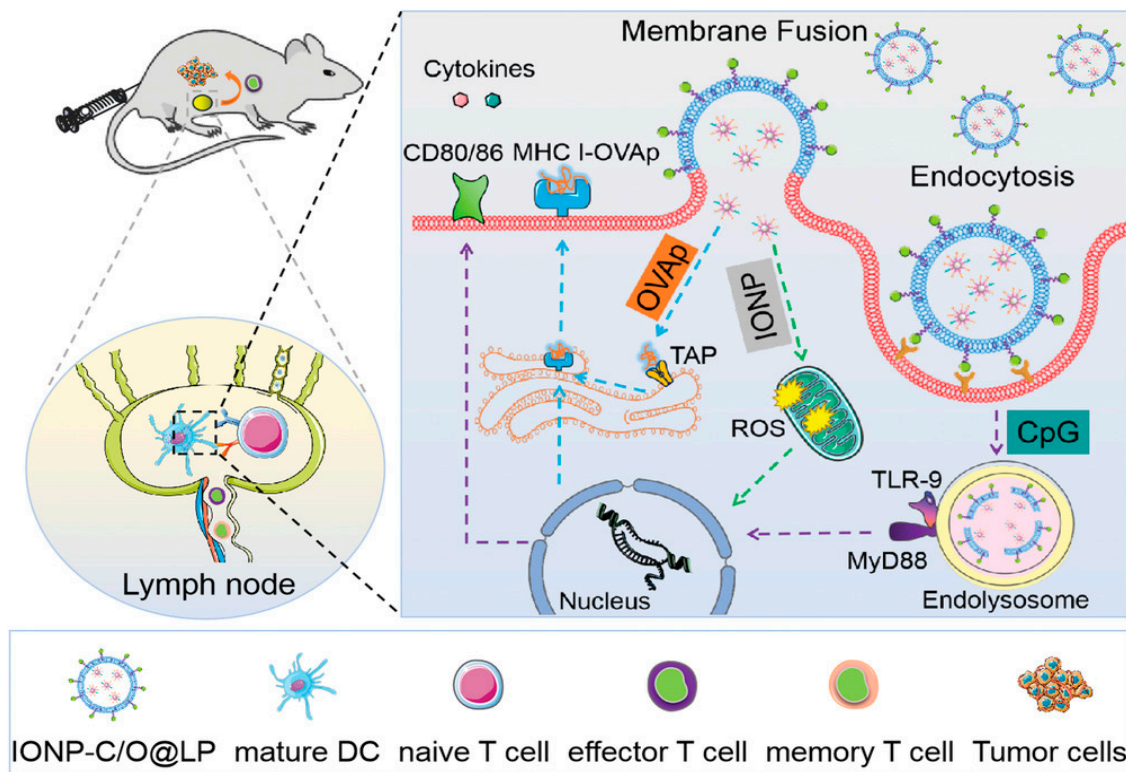


Figure 4. The synergistic effect and immune response elicited by IONP–C/O@LPs. IONPs co–delivered CpG DNA to activate immature DCs, synergistically enhancing immune response and antitumor effect. Reprinted with permission from Ref. [97]. Copyright 2022, Wiley–VCH GmbH.

3.4. IONPs for Combined Phototherapy

Phototherapy, including photothermal therapy treatment (PTT) and photodynamic therapy treatment (PDT), is emerging as a promising strategy for the repeatable and accurate ablation of tumor cells. As potential photothermal materials, IONPs can convert radiated energy into heat to raise the temperature above 42 °C, resulting in the effective killing of tumor cells [98,99]. IONPs also have demonstrated their capabilities to improve the efficiency and safety of this therapeutic strategy by targeting the delivery of photosensitizing agents to tumor sites in animal experiments. For examples, Li et al. demonstrated that IONPs modified with the potent photosensitizer Chlorin e6 could significantly increase the distribution and retention of photosensitizers in mouse subcutaneous melanoma grafts and enhance photodynamic therapy effect [100]. Further, recent research from Yu et al. reported Chlorin e6 loaded through functionalized IONPs linked with glucose showed both target photodynamic efficacy and enhancement in immunogenicity in lung cancer [101]. In addition, IONPs were reported to enhance treatment efficacy in head and neck xenograft tumors and, more importantly, to reduce photosensitizer dose to avoid PDT potential toxicity to normal tissues [102]. However, the advantages of IONPs in targeted phototherapy against tumors have so far only been observed in experimental models, and further verifications of the effectiveness of IONPs in clinical settings are necessary.

IONPs have the potential to combine gene therapy and phototherapy to achieve a synergistic tumor–killing effect. Huang et al. applied IONPs as a bridge to combine PTT and gene therapy. They loaded porous iron oxide nanoparticles (PIONs) with pcDNA3.1–vector–encoding

long noncoding RNA crystallin beta–gamma domain–containing 3 (LNC CRYBG3) to over-express LNC CRYBG3 in tumor cells for degrading the actin cytoskeleton, and inducing cell apoptosis, resulting in the effective destruction of non–small–cell lung cancer cells in vitro and in vivo (Figure 5) [103]. In addition, the success of some IONP–based chemotherapeutics and phototherapy synergistic therapies in animal tumor models also provide the promising of the combination of gene therapy and phototherapy on the basis of IONPs [104,105]. However, it is essential to note that, due to the limited permeability of light to tissues, infrared–light–based PDT and PTT are ineffective in treating deep–seated tumors.

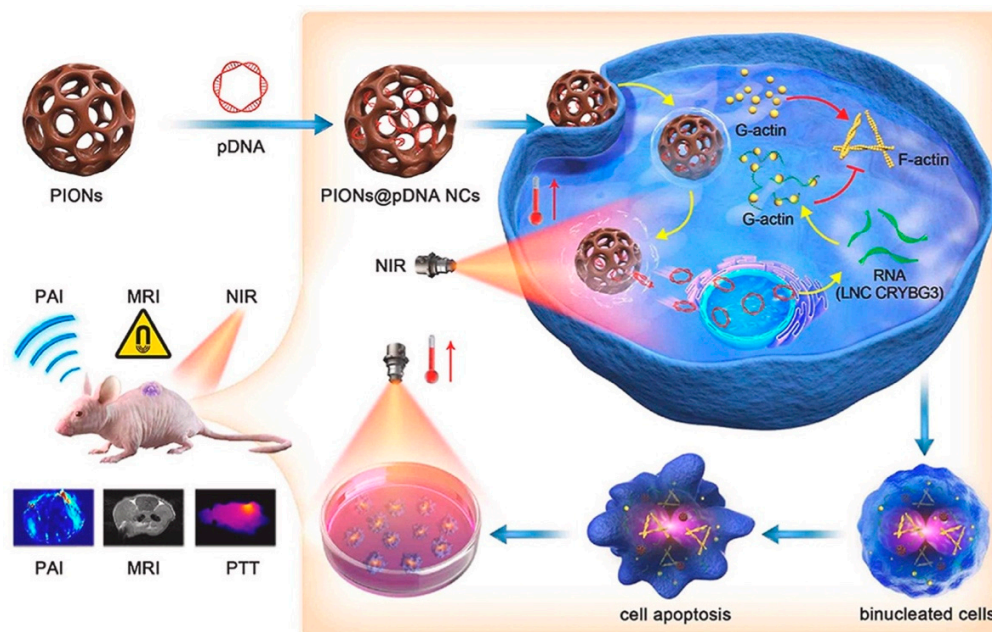


Figure 5. Porous iron oxide nanoparticles (PIONs) loaded with pcDNA3.1–LNC CRYBG3 nanocomplexes (PIONs@pDNA NCs) showed the synergistic ability of MRI, photothermal therapy, and gene therapy to achieve tumor–targeted therapeutics and diagnosis. Reprinted with permission from Ref. [103]. Copyright 2021, Elsevier.

3.5. IONPs for Combined Radiation Therapy

Tumor–targeting radiation therapy is one of the most frequently employed cancer therapies in clinical practice [106]. Definitive radiation therapy consists of high–energy rays that only deliver a lethal dose of radiation to the tumor tissue without damaging the normal tissue surrounding the tumor [107].

IONPs have been extensively studied as radiosensitizers to decrease the radiation dose to normal tissues while increasing the dose to tumor tissues [50,78]. Radiation therapy increases the mitochondrial production of superoxide anions, which convert superoxide dismutase to hydrogen peroxide. Since IONPs can catalyze the conversion of hydrogen peroxide to highly reactive hydroxyl radicals, more reactive oxygen species (ROS) can be generated in tumor cells, thereby enhancing the efficacy of radiotherapy. In addition, surface–functionalized IONPs can enhance the radiosensitization effect and transport drugs to improve the antitumor effect [108]. Forrest et al. developed an IONP–based nanocarrier that could protect the efficient delivery of anti–Ape1 siRNA into brain cancer cells, enabling brain cancer to be sensitive to radiotherapy by knocking down the multifunctional DNA repair enzyme apurinic/uracil glycosylase 1 (Ape1) and, thereby, increasing the antitumor effect and extending the survival of animals, synergizing with radiotherapy [109]. In a separate study, the researchers coated SPIONs with biocompatible, biodegradable coatings of chitosan, PEG, and PEI to achieve the targeted delivery of anti–Ape1 siRNA to pediatric brain tumor cells, reducing Ape1 expression by more than 75% and Ape1 activity by 80% in medulloblastoma and ependymoma cells [110].

3.6. IONPs for Combined Magnetic Hyperthermia Therapy (MHT)

IONP-mediated MHT is a recently proposed cancer treatment [111]. In this strategy, IONPs are applied to generate overheating via Brownian and Neelian relaxations with the assistance of an alternating magnetic field (100–300 kHz), thereby inducing tumor cell apoptosis by heating them to an over-high temperature of 42–46 °C [50,98]. Several studies have applied IONP-mediated MHT with IONP-mediated gene therapy for synergistic effects. For example, Jiang et al. developed a magnetic nucleic acid delivery system comprised of IONPs and cationic lipid-like materials. It could efficiently deliver DNA and siRNA into cells and provide magnetic-guided targeting potential, allowing the combination of gene therapy and MHT [112]. In addition, local heating under MHT exposure increases microvascular tumor permeability, perfusion, and tumor cell membrane permeability, which is crucial for enhancing drug diffusion, cellular absorption, and drug action [98,113].

4. Impacts and Optimization of IONPs for Efficient Cancer Gene Therapy

During the whole process of delivering genes to tumor cells through IONPs, several barriers reduce the delivery efficiency: (i) the stability of nanoparticles; (ii) the accumulation to tumor sites; (iii) the efficiency of intracellular transport; (iv) the gene endosomal escape and further expression; and (v) short blood circulation and quick clearance by the immune system, which is closely related to the therapeutic efficiency of gene therapy [114–117]. Hence, further improvements for IONPs to overcome these barriers are highly required. Several vital aspects that determine the efficiency and safety of using IONPs for cancer gene therapy are discussed in the following section.

4.1. The Stability

Bare IONPs are easily able to aggregate into micrometer-sized clusters in the physiological environment, due to functional group interaction, as well as magnetic, and van der Waals forces [118]. The high surface charge also leads to the agglomeration after the nanoparticles are refined to the nanoscale [82]. Therefore, further modifications of IONPs to ensure colloidal stability are necessary, which is vital for both the delivery efficiency and the safety issues. Surface modification of IONPs with the same electronic charge is one of the major strategies to stabilize IONPs. This strategy can lead to repulsion between nanoparticles due to the electrostatic force, thus benefiting the improvement of nanoparticles' dispersibility in aqueous solution [115]. For example, several polymers, such as chitosan [119,120], PEI [121,122], and PEG [123], have been applied for improving the colloidal stability of IONPs through the enhancement of electrostatic repulsion between nanoparticles.

In addition, generating repulsive steric forces between nanoparticles through surface modification using some long-chain molecules is another strategy to augment the colloidal stability of IONPs. The long-chain polymers attached to the surface of IONPs can increase the absolute value of the electric double layer on the surface of the nanoparticles and enhance the repulsive force between the particles to produce steric protection [124]. For instance, surface modification of IONPs with a methoxy-terminated PEG chain (5000 Da) showed no sign of aggregation for four months in deionized water at room temperature [125]. Long-chain molecules coating IONPs provided nanoparticles with stability through the optimization of the steric properties, further enhancing the repulsion between nanoparticles [126].

The adsorption of biomacromolecules on the surface of IONPs is another challenge impacting the tumor-targeted gene delivery efficiency. For example, IONPs are usually modified to a positive charge in the surface for the efficient loading of nucleic acid drugs. However, these positively charged nanocomplexes are easily adsorbed with the negatively charged plasma proteins in blood circulation after administration, which is known as the formation of protein corona on nanoparticles [127–130]. The formation of protein corona is believed to negatively affect the circulation time and the delivery efficiency

of payloads [131–133]. For example, the interaction between nanoparticles and plasma proteins may alter the uptake and clearance of nanoparticles, thereby affecting the delivery efficiency. It was observed that the protein corona of SPIONs increased the endothelial permeability and uptake of endothelial cells [134]. The increase in hydrodynamic size provoked by the formulation of the protein corona also was reported to drive uptake mechanisms, such as macropinocytosis, further influencing the uptake of nanoparticles [135]. Moreover, the adsorption of plasma proteins on nanoparticles may also induce preferential cellular uptake by immune cells through the recognition of specific complement proteins in the corona, thus decreasing the biodistribution of nanoparticles in tumor cells and resulting in a rapid clearance of nanoparticles [136]. In addition, the adsorption of plasma protein or other kinds of biomacromolecules on IONPs may decrease stability and induce the aggregation of IONPs into micron-sized clusters [137]. For example, Safi et al. observed that the formation of protein corona had significant impacts on the dispersibility of IONPs in biological fluids [138].

Therefore, adopting surface modification to reduce the formation of protein corona on the surface of IONPs is of great significance to reduce clearance by the immune system, increase the blood circulation time, and improve the colloidal stability in biological fluids. For instance, Groult et al. showed that surface modification using phosphatidylcholine could prolong the circulation time and enhance the stability of IONPs due to the resistance of the protein's adsorption [139]. In addition, PEG with high molecular weight was reported to reduce protein adsorption and non-specific uptake by macrophage cells, assisting IONPs escaping from the reticular-endothelial system for a long blood circulation half-life [140].

4.2. The Toxicity Induced by Functional Modification

The toxicity of IONP carriers remains a significant concern, and the modification materials play an important role in the toxicity of IONP-based vectors [70,141]. For uncoated IONPs, the LD-50 ranges from 300 to 600 mg kg⁻¹. However, when their surface was coated with carboxydextran, the LD-50 value changed to 35 mmol kg⁻¹, while it increased to 2000–6000 mg kg⁻¹ when coated with stable and biocompatible dextran molecules [142,143]. In recent years, combining iron oxide cores with different coating molecules has greatly improved gene drug delivery to tumor sites. However, due to their varying toxicities, degradation rates, and pharmacokinetic properties, the study of vector toxicity has become more complex and crucial.

It is common practice to improve gene transfection efficiency by grafting PEI, the “golden standard”, onto IONPs. However, due to its high positive charge density, PEI modification alone would damage the cell membrane and induce cytotoxicity [144]. Therefore, Kievit et al. constructed a PEI-PEG copolymer by grafting PEG to low-molecular-weight PEI. This copolymer provided a physical barrier between the cells and the PEI, thereby reducing the potential toxicity of IONPs. Furthermore, it is essential to note that the design of this PEI-PEG-grafted chitosan had little impact on the magnetism and relaxivity of the iron oxide core, thereby endowing the platform with the dual benefits of gene delivery and in vivo imaging [54].

4.3. The Targeting Ability

Rapidly growing tumors develop intricate vascular structures that provide sufficient nutrients and oxygen to support tumor growth, resulting in a unique, perforated endothelial structure surrounding the tumor. This structure is highly permeable to IONPs, and it can facilitate the passive targeting of IONPs to solid tumors through the EPR effect [145]. In addition, the nanocore size and shape of IONPs play a crucial role in transporting genes into tumor cells.

It is believed that the optimal diameter of nanoparticles for cancer treatment should be between 10 and 100 nm [146–148]. When the diameter of IONPs is less than 10 nm, it is simple for them to pass through the tight endothelial junction and be eliminated by the kidneys' first-pass elimination [149]. While penetrating deeply into the perivascular

region of the tumor, the retention time of these small-sized IONPs may be brief because they are easily pushed out of the tumor by hydraulic forces. IONPs with a diameter over 100 nm are readily isolated by the spleen and liver and quickly absorbed by the mononuclear phagocytosis system [149]. Notably, nanoparticles larger than 100 nm are predominantly trapped in the extracellular space, which is not conducive to gene targeting in cancer cells [150,151]. The effect of tumor cell uptake correlates closely with the efficacy of gene therapy. Compared to larger nanoparticles, nanoparticles with a diameter of less than 50 nm and smaller nanointerfaces that form strong interactions by binding to cluster receptors on the cell membrane tend to have a higher uptake efficiency [134,152].

The regulation of nanoparticle shape is also crucial for enhancing the targeting efficacy of carriers, and an increasing number of studies suggests that adjusting nanoparticle shape can improve tumor targeting efficiency [150,153–155]. In the past decades, spherical nanoparticle carriers were the predominant shape of anticancer drug carriers due to their advantages, such as ease of fabrication. However, several reports have shown the promise of non-spherical nanocarriers have shown increasing promise in anticancer drug delivery [156,157]. Since different aspect ratios can affect the diffusivity of nanomaterials through pores and porous media, Vikash et al. designed and developed nanospheres and nanorods with tunable shapes but the same surface coating and discovered that nanorods excelled at passing through porous media and targeting tumors in vivo (Figure 6) [158].

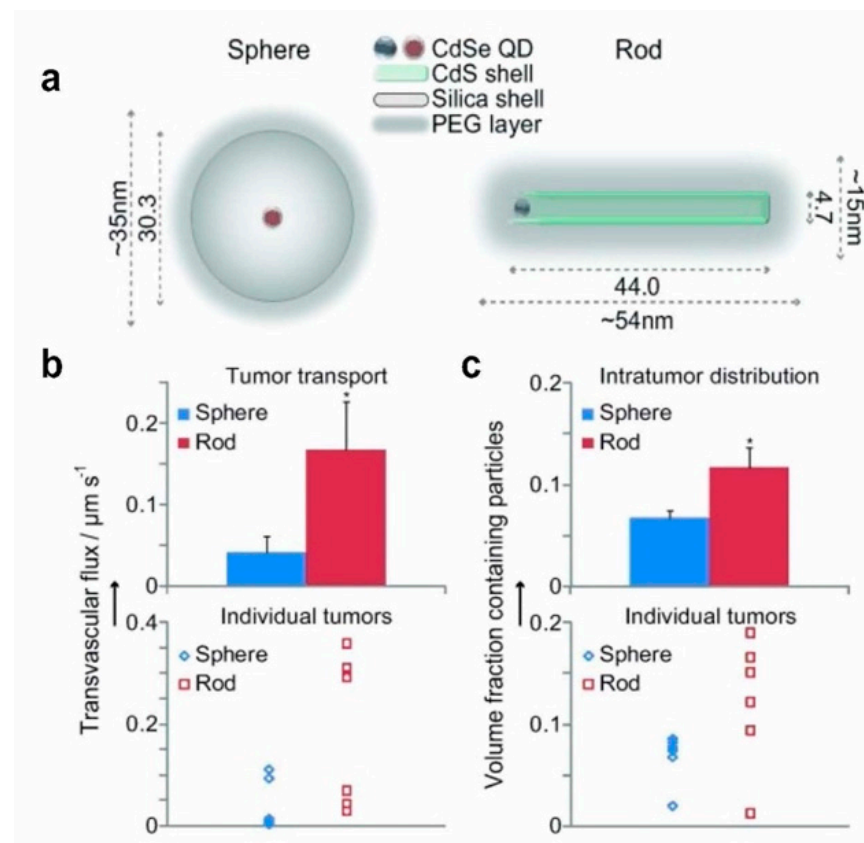


Figure 6. The effect of nanoparticle shape on tumor targeting. (a) Schematic diagram of nanospheres and nanorods. (b) Transvascular transport rates of orthotopic E0771 mammary tumors in mice. Nanorods were transported 4.1 times faster on container walls than nanospheres. (c) Nanoparticle distribution in mouse orthotopic E0771 mammary tumors. Nanorods penetrated 1.7 times the volume of distribution of nanospheres. Reprinted with permission from Ref. [158]. Copyright 2011, Wiley–VCH.

By extending the circulation time of gene-carrying IONPs, it is possible to increase nanoparticle accumulation at tumor sites. The particle shape significantly affects the hy-

hydrodynamic behavior, influencing the circulation time. High-aspect-ratio nanoparticles can conform to blood flow and reduce collisions with vessel walls, resulting in a longer half-life in circulation. In addition, such nanoparticles can increase the probability of particle attachment to vascular walls and improve the interaction between receptor-targeting ligands, thereby facilitating tumor targeting (Figure 7) [159].

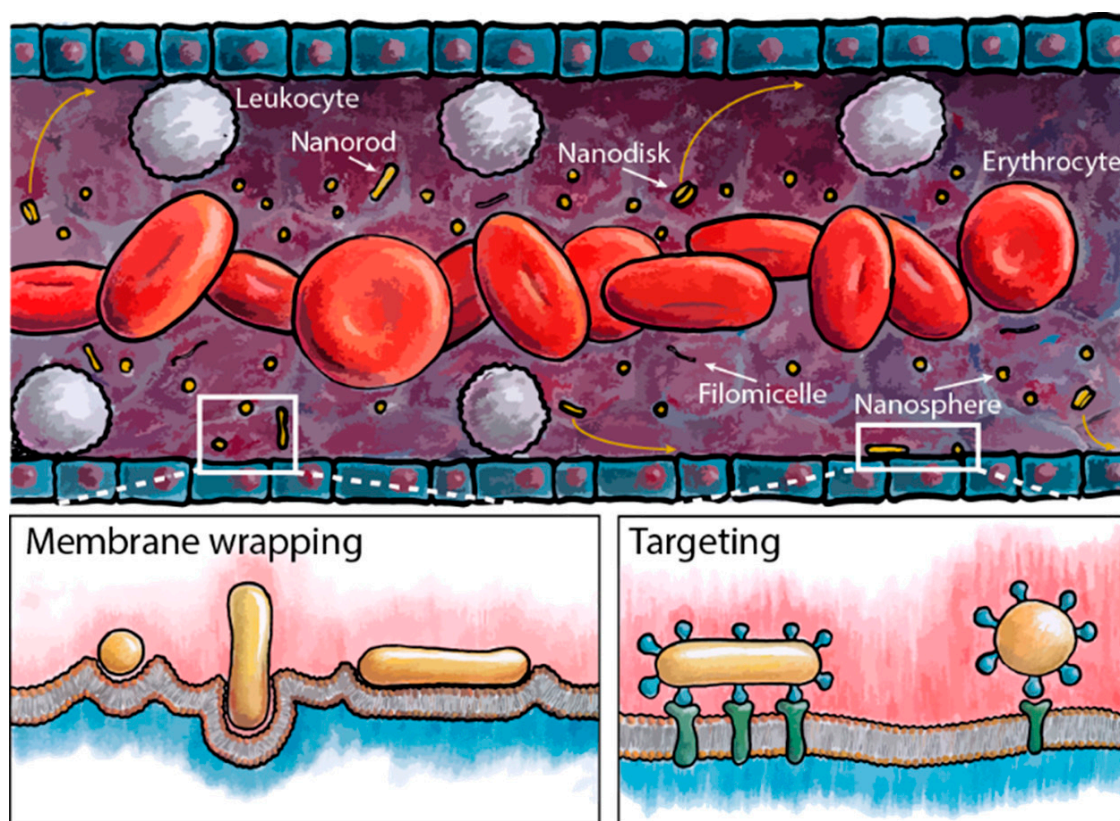


Figure 7. The size and shape of nanoparticles play a crucial role on the hydrodynamic behavior of particles in circulation, including the processes of membrane wrapping and targeting. Reprinted with permission from Ref. [159]. Copyright 2017, American Chemical Society.

Park Ji-Ho et al. designed a dextran-encapsulated iron oxide chain-like aggregate, also known as a nanoworm. The magnetic nanoparticles can be aligned with the assistance of high-molecular-weight dextran chains, taking advantages of high aspect ratio. They discovered that the elongated structure increased the nanoparticles' circulation time, their ability to attach to tumors *in vitro* via multivalent interactions with cell surface receptors, and their passive accumulation at the tumor site [157]. Other studies have demonstrated that extending nanoparticles in a one-dimensional direction can help them avoid natural elimination and achieve a longer circulation time, which is crucial for optimizing the shape of IONPs to improve their efficacy [160,161].

Malignant cells exhibit altered gene and protein expressions, such as overexpression of G-protein-coupled receptors, growth factor receptors, interleukins, transferrin, and polysaccharides, frequently used as targets for the active targeted delivery of functionalized carriers, resulting in enhanced drug delivery at the tumor site [162,163]. It is difficult for bare IONPs to rely solely on the EPR effect to deliver nucleic acid drugs to tumor growth sites such as brain tumors. However, such a situation can be improved to a certain extent under an external magnetic field. Active targeting based on the precise recognition of targeting ligands and their cognate receptors provides additional opportunities for IONP-based drug delivery [164]. Commonly employed targeting ligands in modifying IONPs include peptides, antibodies, aptamers, and small molecules, such as biotin, folic acid, and carbo-

hydrates. Table 2 summarizes current active targeting modification strategies based on IONPs for the delivery of drugs to various drug sites. The active targeting modification strategies can not only improve the efficiency of tumor targeting but it can also prevent damage to normal cells and tissues caused by off-target effects during drug delivery, thereby enhancing the safety of gene therapy.

Table 2. Modification strategies for enhancing active tumor targeting of IONPs.

Modification Strategies	Tumor Models	Advantages	References
Transferrin	Orthotopic 4T1 breast cancer	Tumor retention levels 6 times higher than non-targeted nanoparticles	[165]
Wheat germ agglutinin	MDA-MB-231 breast cancer cells in vitro	Cancer cell death increased by about 2.5-fold	[166]
Folic acid cyclic Arg-Gly-Asp-D-Tyr-Lys	Orthotopic C6 glioma	Uptake enhancement through a combination of dual targets.	[167]
c(RGDyK), d-glucosamine	Xenografted tumor of 4T1 breast cancer	Tumor site accumulation and penetration depth increased	[168]
Monoclonal antibodies	Xenografted tumor of H460 lung cancer	In vivo ultrasound energy deposition significantly improved	[169]
PEGylated amphiphilic triblock copolymer	Xenografted tumor of U87MG glioma	Rapid clearance of the reticuloendothelial system avoided	[170]
Polyvinyl alcohol and Zn/Al-layered double hydroxide	HepG2 liver cancer cells in vitro	Antitumor ability increased No cytotoxic to 3T3 fibroblast cell	[171]

4.4. Intelligent Drug Delivery Based on IONPs

In recent years, intelligent drug delivery systems tailored to the tumor microenvironment (TME), such as acidity, hypoxia, and enzyme imbalance, have provided a more efficient drug delivery strategy towards tumors. This system can transform the carrier's invisible surface into tumor-targeting surfaces for intelligent drug delivery, achieving responsive drug release based on tumor and microenvironment characteristics [172–174].

It has been reported that tumor cells have a different energy metabolism pattern in comparison with normal cells. They acquire energy mainly through anaerobic glycolysis due to the Warburg effect and generate large amounts of lactate, ATP hydrolyzate hydrogen ions, and carbon dioxide in tumor sites, consequently leading to the acidification of TME with a lower pH value (6.5–6.8) than healthy tissues [175,176]. This acidic TME provides an important target for tumor-specific diagnosis and treatment.

Based on the weak acidity of TME, certain pH-sensitive materials have been applied as surface modifications on nanoparticles to develop intelligent drug carriers [175,177]. Cao et al. designed a novel pH-responsive surface-modified single-walled carbon nanotube (SWCNT) and synthesized SWCNT–PB (SPB) to deliver DOX and survivin siRNA synergistically. When the drug-loaded nanocarriers were internalized by cells and encountered acidic endosomes or lysosomes, DOX and survivin siRNA adsorbed on SWCNTs completed the drug release via a mechanism triggered by the protonation of SPB, diffusing from lysosomes to the middle of the cytoplasm. When loaded on SPB, siRNA and DOX could be released efficiently into the cytoplasm and nucleus of A549 cells and exhibited potent antitumor effects in vitro and in vivo (Figure 8) [178].

Together with IONPs, stimulation-independent cationic polymers, such as PEI and PEG, can efficiently achieve gene delivery in tumor cells. However, the rate of dissociation between genes and carriers is limited, and premature dissociation from carriers may result in acid hydrolysis or enzymatic degradation. In contrast, stimulus-dependent materials with high responses to biological stimuli can transform the physicochemical properties of the carrier from a tightly complexed state with genes to a decomposed state in response to stimuli provided in the endosome and cytoplasm, allowing the production of many structurally intact and highly active gene drugs. In addition, the gene and the carrier

cannot be recombined, making initiating the gene therapy procedure challenging. For instance, siRNA must combine with RISC in a free state in the cytoplasm to initiate RNA interference. Therefore, the molecular affinity between the surface-modified responsive materials of IONPs and genes should be irreversible [179,180]. The transformation of genes and polymers from complexation to decomposition in response to tumor-site-specific stimuli is the rate-limiting step in intelligent gene delivery.

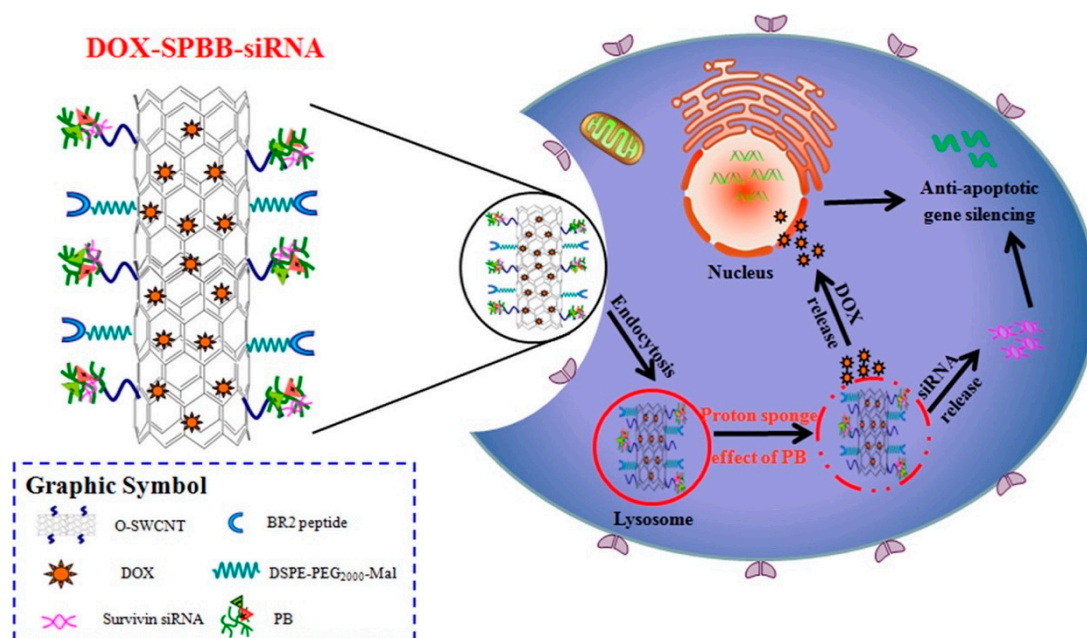


Figure 8. DOX–SPBB–siRNA nanocarriers release DOX and siRNA synergistically in A549 lung cancer cells according to the weak acidity of the tumor microenvironment. Reprinted with permission from Ref. [178]. Copyright 2019, American Chemical Society.

The toxicity of smart, responsive materials used for the surface modification of IONPs is an essential factor that cannot be overlooked. The toxicity of the carrier can be affected by the molecular weight, cation density, morphology, polymer-to-nucleic acid ratio, and biodegradability of the surface-modifying material. In order to improve the efficiency of gene delivery, for instance, specific surface modification strategies have a high molecular weight, cation density, or N/P ratio, which increases vector toxicity and non-specific gene silencing [181]. Therefore, optimizing the minimal *in vivo* and *in vitro* toxicity protocols for gene therapy based on the molecular properties of various coating materials while simultaneously improving gene-targeted tumor delivery is of utmost importance.

5. Conclusions and Outlook

The magnetic responsiveness, good biocompatibility, ease of functional modification, and controllable synthesis of IONPs have enabled the possibility of using IONPs as vehicles for the targeted delivery of a variety of nucleic acid drugs targeting tumor tissues. In addition, the versatility of IONPs has further allowed the combination therapy of gene therapy with some other treatments, showing synergistic effects.

Despite the promising potential of IONP-associated tumor therapy demonstrated in animal studies, the reported clinic trials of this strategy, to the best of our knowledge, are currently limited. IONPs have been widely studied as a contrast agent for magnetic resonance imaging in clinical trials, such as in the diagnosis of pancreatic cancer (NCT00920023), breast cancer (NCT03243435), and thyroid cancer (NCT01927887). IONPs have also been proved by the US Food and Drug Administration (FDA) for the iron replacement therapy of anemia [88]. These clinical applications of IONPs, in addition to the successful results

demonstrated in animal models, may suggest the potential translation of IONP-associated tumor therapy to the clinical bench.

However, there are still some challenges for the application of IONPs to deliver genes to cancer cells. Bare IONPs are generally regarded as nanomaterials with good biocompatibility and safety, but their surface modification may bring the risk of cytotoxicity. In addition, surface modifications of IONPs have demonstrated the advantages of offering various functions, but the magnetic response of IONPs may be affected, thus influencing the magnet targeting efficacy [149,182]. Therefore, it is essential to have further research on the surface-modified materials of IONPs. Moreover, many reports have demonstrated the tumor targeting ability of IONPs, but few studies had focused on the retention time of IONPs in tumors sites. Further improvements in the retention time of IONPs in tumor sites is still worth noting. In addition, since the size and shape of IONPs have a significant impact on drug delivery efficiency, large-amount production of IONPs with uniform and controlled sizes and shapes is a challenge.

In recent years, stem cells have been applied for targeting delivery of gene-loaded IONPs, showing attractive advantages in more specific tumor targeting and biocompatibility, which provide a novel strategy using IONPs for tumor-targeted gene therapy [183]. With the continues advances in materials science, nanotechnology, biological science, and gene therapy, it is believed that the development of an IONP-based delivery platform can be continuously improved and endowed with additional capabilities in cancer treatment.

Author Contributions: J.G. designed and constructed the manuscript. J.Z. wrote the manuscript. T.Z. revised the manuscript. All authors have read and agreed to the published version of the manuscript.

Funding: This work was supported by the Natural Science Foundation of Zhejiang Province (LD22H300002), the National Natural Science Foundation of China (81703423), and the Fundamental Research Funds for the Central Universities (226-2022-00125).

Data Availability Statement: Not applicable.

Conflicts of Interest: The authors declare no conflict of interest.

References

1. Brenner, M.K.; Gottschalk, S.; Leen, A.M.; Vera, J.F. Is cancer gene therapy an empty suit? *Lancet Oncol.* **2013**, *14*, e447–e456. [[CrossRef](#)]
2. Xin, Y.; Huang, M.; Guo, W.W.; Huang, Q.; Zhang, L.Z.; Jiang, G. Nano-based delivery of RNAi in cancer therapy. *Mol. Cancer* **2017**, *16*, 134. [[CrossRef](#)] [[PubMed](#)]
3. Larsson, M.; Huang, W.T.; Liu, D.M.; Losic, D. Local co-administration of gene-silencing RNA and drugs in cancer therapy: State-of-the art and therapeutic potential. *Cancer Treat. Rev.* **2017**, *55*, 128–135. [[CrossRef](#)]
4. Nastiuk, K.L.; Krolewski, J.J. Opportunities and challenges in combination gene cancer therapy. *Adv. Drug Deliv. Rev.* **2016**, *98*, 35–40. [[CrossRef](#)]
5. Roma-Rodrigues, C.; Rivas-Garcia, L.; Baptista, P.V.; Fernandes, A.R. Gene therapy in cancer treatment: Why go nano? *Pharmaceutics* **2020**, *12*, 233. [[CrossRef](#)] [[PubMed](#)]
6. High, K.A.; Roncarolo, M.G. Gene therapy. *N. Engl. J. Med.* **2019**, *381*, 455–464. [[CrossRef](#)]
7. Villanueva, M.T. Gene therapy: Gene therapy before the cradle. *Nat. Rev. Drug Discov.* **2018**, *17*, 619. [[CrossRef](#)] [[PubMed](#)]
8. Daley, J. Four success stories in gene therapy. *Nature* **2021**. [[CrossRef](#)] [[PubMed](#)]
9. Luo, X.; Zhao, W.; Li, B.; Zhang, X.; Zhang, C.; Bratasz, A.; Deng, B.; McComb, D.W.; Dong, Y. Co-delivery of mRNA and SPIONs through amino-ester nanomaterials. *Nano Res.* **2018**, *11*, 5596–5603. [[CrossRef](#)] [[PubMed](#)]
10. Berraondo, P.; Martini, P.G.V.; Avila, M.A.; Fontanellas, A. Messenger RNA therapy for rare genetic metabolic diseases. *Gut* **2019**, *68*, 1323–1330. [[CrossRef](#)]
11. Kim, B.; Park, J.H.; Sailor, M.J. Rekindling RNAi therapy: Materials design requirements for in vivo siRNA delivery. *Adv. Mater.* **2019**, *31*, e1903637. [[CrossRef](#)] [[PubMed](#)]
12. Collins, F.S.; Gottlieb, S. The next phase of human gene-therapy oversight. *N. Engl. J. Med.* **2018**, *379*, 1393–1395. [[CrossRef](#)] [[PubMed](#)]
13. Dowdy, S.F. Controlling CRISPR–Cas9 gene editing. *N. Engl. J. Med.* **2019**, *381*, 289–290. [[CrossRef](#)] [[PubMed](#)]
14. Zlotorynski, E. Genome engineering: NHEJ and CRISPR–Cas9 improve gene therapy. *Nat. Rev. Mol. Cell Biol.* **2016**, *18*, 4. [[CrossRef](#)] [[PubMed](#)]

15. Feiner-Gracia, N.; Olea, R.A.; Fitzner, R.; El Boujnouni, N.; van Asbeck, A.H.; Brock, R.; Albertazzi, L. Super-resolution imaging of structure, molecular composition, and stability of single oligonucleotide polyplexes. *Nano Lett.* **2019**, *19*, 2784–2792. [[CrossRef](#)] [[PubMed](#)]
16. Wang, J.; Meng, F.; Kim, B.K.; Ke, X.; Yeo, Y. In-vitro and in-vivo difference in gene delivery by lithocholic acid–polyethyleneimine conjugate. *Biomaterials* **2019**, *217*, 119296. [[CrossRef](#)] [[PubMed](#)]
17. Karjoo, Z.; Chen, X.; Hatefi, A. Progress and problems with the use of suicide genes for targeted cancer therapy. *Adv. Drug Deliv. Rev.* **2016**, *99*, 113–128. [[CrossRef](#)] [[PubMed](#)]
18. Wang, D.; Tai, P.W.L.; Gao, G. Adeno-associated virus vector as a platform for gene therapy delivery. *Nat. Rev. Drug Discov.* **2019**, *18*, 358–378. [[CrossRef](#)] [[PubMed](#)]
19. Li, C.; Samulski, R.J. Engineering adeno-associated virus vectors for gene therapy. *Nat. Rev. Genet.* **2020**, *21*, 255–272. [[CrossRef](#)] [[PubMed](#)]
20. The Committee for Advanced Therapies (CAT); CAT Scientific Secretariat; Schneider, C.K.; Salmikangas, P.; Jilma, B.; Flamion, B.; Todorova, L.R.; Paphitou, A.; Haunerova, I.; Maimets, T.; et al. Challenges with advanced therapy medicinal products and how to meet them. *Nat. Rev. Drug Discov.* **2010**, *9*, 195–201. [[CrossRef](#)] [[PubMed](#)]
21. Paunovska, K.; Loughrey, D.; Dahلمان, J.E. Drug delivery systems for RNA therapeutics. *Nat. Rev. Genet.* **2022**, *23*, 265–280. [[CrossRef](#)] [[PubMed](#)]
22. Dirisala, A.; Uchida, S.; Tockary, T.A.; Yoshinaga, N.; Li, J.; Osawa, S.; Gorantla, L.; Fukushima, S.; Osada, K.; Kataoka, K. Precise tuning of disulphide crosslinking in mRNA polyplex micelles for optimising extracellular and intracellular nuclease tolerability. *J. Drug Target.* **2019**, *27*, 670–680. [[CrossRef](#)] [[PubMed](#)]
23. Chen, Y.; Gao, D.Y.; Huang, L. In vivo delivery of miRNAs for cancer therapy: Challenges and strategies. *Adv. Drug Deliv. Rev.* **2015**, *81*, 128–141. [[CrossRef](#)] [[PubMed](#)]
24. Thakor, A.S.; Gambhir, S.S. Nanooncology: The future of cancer diagnosis and therapy. *CA Cancer J. Clin.* **2013**, *63*, 395–418. [[CrossRef](#)] [[PubMed](#)]
25. Venditti, C.P. Safety questions for AAV gene therapy. *Nat. Biotechnol.* **2021**, *39*, 24–26. [[CrossRef](#)]
26. Zhao, Z.; Anselmo, A.C.; Mitragotri, S. Viral vector-based gene therapies in the clinic. *Bioeng. Transl. Med.* **2022**, *7*, e10258. [[CrossRef](#)]
27. Santiago-Ortiz, J.L.; Schaffer, D.V. Adeno-associated virus (AAV) vectors in cancer gene therapy. *J. Control. Release* **2016**, *240*, 287–301. [[CrossRef](#)]
28. Kaiser, J. How safe is a popular gene therapy vector? *Science* **2020**, *367*, 131. [[CrossRef](#)]
29. Kaepfel, C.; Beattie, S.G.; Fronza, R.; van Logtenstein, R.; Salmon, F.; Schmidt, S.; Wolf, S.; Nowrouzi, A.; Glimm, H.; von Kalle, C.; et al. A largely random AAV integration profile after LPLD gene therapy. *Nat. Med.* **2013**, *19*, 889–891. [[CrossRef](#)]
30. Chowdhury, E.A.; Meno–Tetang, G.; Chang, H.Y.; Wu, S.; Huang, H.W.; Jamier, T.; Chandran, J.; Shah, D.K. Current progress and limitations of AAV mediated delivery of protein therapeutic genes and the importance of developing quantitative pharmacokinetic/pharmacodynamic (PK/PD) models. *Adv. Drug Deliv. Rev.* **2021**, *170*, 214–237. [[CrossRef](#)]
31. Bariwal, J.; Ma, H.; Altenberg, G.A.; Liang, H. Nanodiscs: A versatile nanocarrier platform for cancer diagnosis and treatment. *Chem. Soc. Rev.* **2022**, *51*, 1702–1728. [[CrossRef](#)]
32. Vaughan, H.J.; Green, J.J.; Tzeng, S.Y. Cancer-targeting nanoparticles for combinatorial nucleic acid delivery. *Adv. Mater.* **2020**, *32*, e1901081. [[CrossRef](#)] [[PubMed](#)]
33. Yin, H.; Kanasty, R.L.; Eltoukhy, A.A.; Vegas, A.J.; Dorkin, J.R.; Anderson, D.G. Non-viral vectors for gene-based therapy. *Nat. Rev. Genet.* **2014**, *15*, 541–555. [[CrossRef](#)]
34. Yan, Y.; Liu, X.Y.; Lu, A.; Wang, X.Y.; Jiang, L.X.; Wang, J.C. Non-viral vectors for RNA delivery. *J. Control. Release* **2022**, *342*, 241–279. [[CrossRef](#)] [[PubMed](#)]
35. Dirisala, A.; Osada, K.; Chen, Q.; Tockary, T.A.; Machitani, K.; Osawa, S.; Liu, X.; Ishii, T.; Miyata, K.; Oba, M.; et al. Optimized rod length of polyplex micelles for maximizing transfection efficiency and their performance in systemic gene therapy against stroma–rich pancreatic tumors. *Biomaterials* **2014**, *35*, 5359–5368. [[CrossRef](#)] [[PubMed](#)]
36. Uchida, S.; Kinoh, H.; Ishii, T.; Matsui, A.; Tockary, T.A.; Takeda, K.M.; Uchida, H.; Osada, K.; Itaka, K.; Kataoka, K. Systemic delivery of messenger RNA for the treatment of pancreatic cancer using polyplex nanomicelles with a cholesterol moiety. *Biomaterials* **2016**, *82*, 221–228. [[CrossRef](#)]
37. Chen, Q.; Osada, K.; Ishii, T.; Oba, M.; Uchida, S.; Tockary, T.A.; Endo, T.; Ge, Z.; Kinoh, H.; Kano, M.R.; et al. Homo-cationer integration into PEGylated polyplex micelle from block-cationer for systemic anti–angiogenic gene therapy for fibrotic pancreatic tumors. *Biomaterials* **2012**, *33*, 4722–4730. [[CrossRef](#)]
38. Tockary, T.A.; Foo, W.; Dirisala, A.; Chen, Q.; Uchida, S.; Osawa, S.; Mochida, Y.; Liu, X.; Kinoh, H.; Cabral, H.; et al. Single-stranded DNA-packaged polyplex micelle as adeno–associated–virus–inspired compact vector to systemically target stroma-rich pancreatic cancer. *ACS Nano* **2019**, *13*, 12732–12742. [[CrossRef](#)]
39. Sukumar, U.K.; Packirisamy, G. Bioactive core-shell nanofiber hybrid scaffold for efficient suicide gene transfection and subsequent time resolved delivery of prodrug for anticancer therapy. *ACS Appl. Mater. Interfaces* **2015**, *7*, 18717–18731. [[CrossRef](#)]
40. Duan, X.; Wang, P.; Men, K.; Gao, X.; Huang, M.; Gou, M.; Chen, L.; Qian, Z.; Wei, Y. Treating colon cancer with a suicide gene delivered by self-assembled cationic MPEG–PCL micelles. *Nanoscale* **2012**, *4*, 2400–2407. [[CrossRef](#)]

41. Dirisala, A.; Uchida, S.; Toh, K.; Li, J.; Osawa, S.; Tockary, T.A.; Liu, X.; Abbasi, S.; Hayashi, K.; Mochida, Y.; et al. Transient stealth coating of liver sinusoidal wall by anchoring two-armed PEG for retargeting nanomedicines. *Sci. Adv.* **2020**, *6*, eabb8133. [[CrossRef](#)] [[PubMed](#)]
42. Jiang, T.; Qiao, Y.; Ruan, W.; Zhang, D.; Yang, Q.; Wang, G.; Chen, Q.; Zhu, F.; Yin, J.; Zou, Y.; et al. Cation-Free siRNA micelles as effective drug delivery platform and potent RNAi nanomedicines for glioblastoma therapy. *Adv. Mater.* **2021**, *33*, e2104779. [[CrossRef](#)] [[PubMed](#)]
43. Van Haasteren, J.; Li, J.; Scheideler, O.J.; Murthy, N.; Schaffer, D.V. The delivery challenge: Fulfilling the promise of therapeutic genome editing. *Nat. Biotechnol.* **2020**, *38*, 845–855. [[CrossRef](#)] [[PubMed](#)]
44. Tsoi, K.M.; MacParland, S.A.; Ma, X.Z.; Spetzler, V.N.; Echeverri, J.; Ouyang, B.; Fadel, S.M.; Sykes, E.A.; Goldaracena, N.; Kathis, J.M.; et al. Mechanism of hard-nanomaterial clearance by the liver. *Nat. Mater.* **2016**, *15*, 1212–1221. [[CrossRef](#)] [[PubMed](#)]
45. Jia, H.R.; Zhu, Y.X.; Duan, Q.Y.; Chen, Z.; Wu, F.G. Nanomaterials meet zebrafish: Toxicity evaluation and drug delivery applications. *J. Control. Release* **2019**, *311–312*, 301–318. [[CrossRef](#)]
46. Khan, A.R.; Yang, X.; Du, X.; Yang, H.; Liu, Y.; Khan, A.Q.; Zhai, G. Chondroitin sulfate derived theranostic and therapeutic nanocarriers for tumor-targeted drug delivery. *Carbohydr. Polym.* **2020**, *233*, 115837. [[CrossRef](#)]
47. Karaosmanoglu, S.; Zhou, M.; Shi, B.; Zhang, X.; Williams, G.R.; Chen, X. Carrier-free nanodrugs for safe and effective cancer treatment. *J. Control. Release* **2021**, *329*, 805–832. [[CrossRef](#)]
48. Stanicki, D.; Vangijzegem, T.; Ternad, I.; Laurent, S. An update on the applications and characteristics of magnetic iron oxide nanoparticles for drug delivery. *Expert Opin. Drug Deliv.* **2022**, *19*, 321–335. [[CrossRef](#)]
49. Luther, D.C.; Huang, R.; Jeon, T.; Zhang, X.; Lee, Y.W.; Nagaraj, H.; Rotello, V.M. Delivery of drugs, proteins, and nucleic acids using inorganic nanoparticles. *Adv. Drug Deliv. Rev.* **2020**, *156*, 188–213. [[CrossRef](#)]
50. Tong, S.; Zhu, H.; Bao, G. Magnetic iron oxide nanoparticles for disease detection and therapy. *Mater. Today* **2019**, *31*, 86–99. [[CrossRef](#)]
51. Hola, K.; Markova, Z.; Zoppellaro, G.; Tucek, J.; Zboril, R. Tailored functionalization of iron oxide nanoparticles for MRI, drug delivery, magnetic separation and immobilization of biosubstances. *Biotechnol. Adv.* **2015**, *33*, 1162–1176. [[CrossRef](#)] [[PubMed](#)]
52. Wang, K.; Kievit, F.M.; Sham, J.G.; Jeon, M.; Stephen, Z.R.; Bakthavatsalam, A.; Park, J.O.; Zhang, M. Iron-oxide-based nanovector for tumor targeted siRNA delivery in an orthotopic hepatocellular carcinoma xenograft mouse model. *Small* **2016**, *12*, 477–487. [[CrossRef](#)] [[PubMed](#)]
53. Lin, G.; Huang, J.; Zhang, M.; Chen, S.; Zhang, M. Chitosan-crosslinked low molecular weight PEI-conjugated iron oxide nanoparticle for safe and effective DNA delivery to breast cancer cells. *Nanomaterials* **2022**, *12*, 584. [[CrossRef](#)] [[PubMed](#)]
54. Kievit, F.M.; Veisoh, O.; Bhattarai, N.; Fang, C.; Gunn, J.W.; Lee, D.; Ellenbogen, R.G.; Olson, J.M.; Zhang, M. PEI-PEG-chitosan copolymer coated iron oxide nanoparticles for safe gene delivery: Synthesis, complexation, and transfection. *Adv. Funct. Mater.* **2009**, *19*, 2244–2251. [[CrossRef](#)] [[PubMed](#)]
55. Hu, S.H.; Hsieh, T.Y.; Chiang, C.S.; Chen, P.J.; Chen, Y.Y.; Chiu, T.L.; Chen, S.Y. Surfactant-free, lipo-polymersomes stabilized by iron oxide nanoparticles/polymer interlayer for synergistically targeted and magnetically guided gene delivery. *Adv. Healthc. Mater.* **2014**, *3*, 273–282. [[CrossRef](#)]
56. Cao, Y.; Zhang, S.; Ma, M.; Zhang, Y. Fluorinated PEG-PEI coated magnetic nanoparticles for siRNA delivery and CXCR4 knockdown. *Nanomaterials* **2022**, *12*, 1692. [[CrossRef](#)]
57. Jin, L.; Wang, Q.; Chen, J.; Wang, Z.; Xin, H.; Zhang, D. Efficient delivery of therapeutic siRNA by Fe₃O₄ magnetic nanoparticles into oral cancer cells. *Pharmaceutics* **2019**, *11*, 615. [[CrossRef](#)]
58. Dalmina, M.; Pittella, F.; Sierra, J.A.; Souza, G.R.R.; Silva, A.H.; Pasa, A.A.; Creczynski-Pasa, T.B. Magnetically responsive hybrid nanoparticles for in vitro siRNA delivery to breast cancer cells. *Mater. Sci. Eng. C Mater. Biol. Appl.* **2019**, *99*, 1182–1190. [[CrossRef](#)]
59. Panday, R.; Abdalla, A.M.E.; Yu, M.; Li, X.; Ouyang, C.; Yang, G. Functionally modified magnetic nanoparticles for effective siRNA delivery to prostate cancer cells in vitro. *J. Biomater. Appl.* **2020**, *34*, 952–964. [[CrossRef](#)]
60. Luo, X.; Peng, X.; Hou, J.; Wu, S.; Shen, J.; Wang, L. Folic acid-functionalized polyethylenimine superparamagnetic iron oxide nanoparticles as theranostic agents for magnetic resonance imaging and PD-L1 siRNA delivery for gastric cancer. *Int. J. Nanomed.* **2017**, *12*, 5331–5343. [[CrossRef](#)]
61. Yoo, B.; Ghosh, S.K.; Kumar, M.; Moore, A.; Yigit, M.V.; Medarova, Z. Design of nanodrugs for miRNA targeting in tumor cells. *J. Biomed. Nanotechnol.* **2014**, *10*, 1114–1122. [[CrossRef](#)] [[PubMed](#)]
62. Zhang, Y.; Fu, X.; Jia, J.; Wikerholmen, T.; Xi, K.; Kong, Y.; Wang, J.; Chen, H.; Ma, Y.; Li, Z.; et al. Glioblastoma therapy using codelivery of cisplatin and glutathione peroxidase targeting siRNA from iron oxide nanoparticles. *ACS Appl. Mater. Interfaces* **2020**, *12*, 43408–43421. [[CrossRef](#)] [[PubMed](#)]
63. Yang, Z.; Duan, J.; Wang, J.; Liu, Q.; Shang, R.; Yang, X.; Lu, P.; Xia, C.; Wang, L.; Dou, K. Superparamagnetic iron oxide nanoparticles modified with polyethylenimine and galactose for siRNA targeted delivery in hepatocellular carcinoma therapy. *Int. J. Nanomed.* **2018**, *13*, 1851–1865. [[CrossRef](#)]
64. Li, D.; Tang, X.; Pulli, B.; Lin, C.; Zhao, P.; Cheng, J.; Lv, Z.; Yuan, X.; Luo, Q.; Cai, H.; et al. Theranostic nanoparticles based on bioreducible polyethylenimine-coated iron oxide for reduction-responsive gene delivery and magnetic resonance imaging. *Int. J. Nanomed.* **2014**, *9*, 3347–3361. [[CrossRef](#)]
65. Israel, L.L.; Galstyan, A.; Holler, E.; Ljubimova, J.Y. Magnetic iron oxide nanoparticles for imaging, targeting and treatment of primary and metastatic tumors of the brain. *J. Control. Release* **2020**, *320*, 45–62. [[CrossRef](#)] [[PubMed](#)]

66. Hamilton, A.M.; Aidoudi-Ahmed, S.; Sharma, S.; Kotamraju, V.R.; Foster, P.J.; Sugahara, K.N.; Ruoslahti, E.; Rutt, B.K. Nanoparticles coated with the tumor-penetrating peptide iRGD reduce experimental breast cancer metastasis in the brain. *J. Mol. Med.* **2015**, *93*, 991–1001. [[CrossRef](#)] [[PubMed](#)]
67. Zhang, X.; Wu, F.; Men, K.; Huang, R.; Zhou, B.; Zhang, R.; Zou, R.; Yang, L. Modified Fe₃O₄ magnetic nanoparticle delivery of CpG inhibits tumor growth and spontaneous pulmonary metastases to enhance immunotherapy. *Nanoscale Res. Lett.* **2018**, *13*, 240. [[CrossRef](#)] [[PubMed](#)]
68. Maeda, H. Macromolecular therapeutics in cancer treatment: The EPR effect and beyond. *J. Control. Release* **2012**, *164*, 138–144. [[CrossRef](#)] [[PubMed](#)]
69. Stylianopoulos, T. EPR-effect: Utilizing size-dependent nanoparticle delivery to solid tumors. *Ther. Deliv.* **2013**, *4*, 421–423. [[CrossRef](#)]
70. Arami, H.; Khandhar, A.; Liggitt, D.; Krishnan, K.M. In vivo delivery, pharmacokinetics, biodistribution and toxicity of iron oxide nanoparticles. *Chem. Soc. Rev.* **2015**, *44*, 8576–8607. [[CrossRef](#)] [[PubMed](#)]
71. Kamei, K.; Mukai, Y.; Kojima, H.; Yoshikawa, T.; Yoshikawa, M.; Kiyohara, G.; Yamamoto, T.A.; Yoshioka, Y.; Okada, N.; Seino, S.; et al. Direct cell entry of gold/iron-oxide magnetic nanoparticles in adenovirus mediated gene delivery. *Biomaterials* **2009**, *30*, 1809–1814. [[CrossRef](#)] [[PubMed](#)]
72. Marcus, M.; Smith, A.; Maswadeh, A.; Shemesh, Z.; Zak, I.; Motiei, M.; Schori, H.; Margel, S.; Sharoni, A.; Shefi, O. Magnetic targeting of growth factors using iron oxide nanoparticles. *Nanomaterials* **2018**, *8*, 707. [[CrossRef](#)] [[PubMed](#)]
73. Zhao, S.; Yu, X.; Qian, Y.; Chen, W.; Shen, J. Multifunctional magnetic iron oxide nanoparticles: An advanced platform for cancer theranostics. *Theranostics* **2020**, *10*, 6278–6309. [[CrossRef](#)] [[PubMed](#)]
74. Zhi, D.; Yang, T.; Yang, J.; Fu, S.; Zhang, S. Targeting strategies for superparamagnetic iron oxide nanoparticles in cancer therapy. *Acta Biomater.* **2020**, *102*, 13–34. [[CrossRef](#)] [[PubMed](#)]
75. Alphantery, E. Biodistribution and targeting properties of iron oxide nanoparticles for treatments of cancer and iron anemia disease. *Nanotoxicology* **2019**, *13*, 573–596. [[CrossRef](#)] [[PubMed](#)]
76. Ulbrich, K.; Hola, K.; Subr, V.; Bakandritsos, A.; Tucek, J.; Zboril, R. Targeted drug delivery with polymers and magnetic nanoparticles: Covalent and noncovalent approaches, release control, and clinical studies. *Chem. Rev.* **2016**, *116*, 5338–5431. [[CrossRef](#)] [[PubMed](#)]
77. Lee, G.Y.; Qian, W.P.; Wang, L.; Wang, Y.A.; Staley, C.A.; Satpathy, M.; Nie, S.; Mao, H.; Yang, L. Theranostic nanoparticles with controlled release of gemcitabine for targeted therapy and MRI of pancreatic cancer. *ACS Nano* **2013**, *7*, 2078–2089. [[CrossRef](#)] [[PubMed](#)]
78. Lee, N.; Yoo, D.; Ling, D.; Cho, M.H.; Hyeon, T.; Cheon, J. Iron oxide based nanoparticles for multimodal imaging and magnetoresponsive therapy. *Chem. Rev.* **2015**, *115*, 10637–10689. [[CrossRef](#)] [[PubMed](#)]
79. Barrow, M.; Taylor, A.; Murray, P.; Rosseinsky, M.J.; Adams, D.J. Design considerations for the synthesis of polymer coated iron oxide nanoparticles for stem cell labelling and tracking using MRI. *Chem. Soc. Rev.* **2015**, *44*, 6733–6748. [[CrossRef](#)] [[PubMed](#)]
80. Lee, N.; Hyeon, T. Designed synthesis of uniformly sized iron oxide nanoparticles for efficient magnetic resonance imaging contrast agents. *Chem. Soc. Rev.* **2012**, *41*, 2575–2589. [[CrossRef](#)]
81. Ahrens, E.T.; Bulte, J.W. Tracking immune cells in vivo using magnetic resonance imaging. *Nat. Rev. Immunol.* **2013**, *13*, 755–763. [[CrossRef](#)]
82. Low, L.E.; Lim, H.P.; Ong, Y.S.; Siva, S.P.; Sia, C.S.; Goh, B.H.; Chan, E.S.; Tey, B.T. Stimuli-controllable iron oxide nanoparticle assemblies: Design, manipulation and bio-applications. *J. Control. Release* **2022**, *345*, 231–274. [[CrossRef](#)] [[PubMed](#)]
83. Santra, S.; Jativa, S.D.; Kaittanis, C.; Normand, G.; Grimm, J.; Perez, J.M. Gadolinium-encapsulating iron oxide nanoprobe as activatable NMR/MRI contrast agent. *ACS Nano* **2012**, *6*, 7281–7294. [[CrossRef](#)] [[PubMed](#)]
84. Rebolledo, A.F.; Laurent, S.; Calero, M.; Villanueva, A.; Knobel, M.; Marco, J.F.; Tartaj, P. Iron oxide nanosized clusters embedded in porous nanorods: A new colloidal design to enhance capabilities of MRI contrast agents. *ACS Nano* **2010**, *4*, 2095–2103. [[CrossRef](#)] [[PubMed](#)]
85. Wei, H.; Wisniewska, A.; Fan, J.; Harvey, P.; Li, Y.; Wu, V.; Hansen, E.C.; Zhang, J.; Kaul, M.G.; Frey, A.M.; et al. Single-nanometer iron oxide nanoparticles as tissue-permeable MRI contrast agents. *Proc. Natl. Acad. Sci. USA* **2021**, *118*, e2102340118. [[CrossRef](#)]
86. Mahajan, U.M.; Teller, S.; Sandler, M.; Palankar, R.; van den Brandt, C.; Schwaiger, T.; Kuhn, J.P.; Ribback, S.; Glockl, G.; Evert, M.; et al. Tumour-specific delivery of siRNA-coupled superparamagnetic iron oxide nanoparticles, targeted against PLK1, stops progression of pancreatic cancer. *Gut* **2016**, *65*, 1838–1849. [[CrossRef](#)] [[PubMed](#)]
87. Li, B.; Shao, H.; Gao, L.; Li, H.; Sheng, H.; Zhu, L. Nano-drug co-delivery system of natural active ingredients and chemotherapy drugs for cancer treatment: A review. *Drug Deliv.* **2022**, *29*, 2130–2161. [[CrossRef](#)] [[PubMed](#)]
88. Revia, R.A.; Stephen, Z.R.; Zhang, M. Theranostic Nanoparticles for RNA-Based Cancer Treatment. *Acc. Chem. Res.* **2019**, *52*, 1496–1506. [[CrossRef](#)] [[PubMed](#)]
89. Song, Y.; Li, D.; Lu, Y.; Jiang, K.; Yang, Y.; Xu, Y.; Dong, L.; Yan, X.; Ling, D.; Yang, X.; et al. Ferrimagnetic mPEG-b-PHEP copolymer micelles loaded with iron oxide nanocubes and emodin for enhanced magnetic hyperthermia-chemotherapy. *Natl. Sci. Rev.* **2020**, *7*, 723–736. [[CrossRef](#)] [[PubMed](#)]
90. Mai, B.T.; Balakrishnan, P.B.; Barthel, M.J.; Piccardi, F.; Niculaes, D.; Marinaro, F.; Fernandes, S.; Curcio, A.; Kakwere, H.; Autret, G.; et al. Thermoresponsive iron oxide nanocubes for an effective clinical translation of magnetic hyperthermia and heat-mediated chemotherapy. *ACS Appl. Mater. Interfaces* **2019**, *11*, 5727–5739. [[CrossRef](#)] [[PubMed](#)]

91. Mahmoudi, M.; Sant, S.; Wang, B.; Laurent, S.; Sen, T. Superparamagnetic iron oxide nanoparticles (SPIONs): Development, surface modification and applications in chemotherapy. *Adv. Drug Deliv. Rev.* **2011**, *63*, 24–46. [[CrossRef](#)] [[PubMed](#)]
92. Li, Y.; Chen, Y.; Li, J.; Zhang, Z.; Huang, C.; Lian, G.; Yang, K.; Chen, S.; Lin, Y.; Wang, L.; et al. Co-delivery of microRNA-21 antisense oligonucleotides and gemcitabine using nanomedicine for pancreatic cancer therapy. *Cancer Sci.* **2017**, *108*, 1493–1503. [[CrossRef](#)] [[PubMed](#)]
93. Geppert, M.; Himly, M. Iron oxide nanoparticles in bioimaging—An immune perspective. *Front. Immunol.* **2021**, *12*, 688927. [[CrossRef](#)] [[PubMed](#)]
94. Khan, S.; Setua, S.; Kumari, S.; Dan, N.; Massey, A.; Hafeez, B.B.; Yallapu, M.M.; Stiles, Z.E.; Alabkaa, A.; Yue, J.; et al. Superparamagnetic iron oxide nanoparticles of curcumin enhance gemcitabine therapeutic response in pancreatic cancer. *Biomaterials* **2019**, *208*, 83–97. [[CrossRef](#)] [[PubMed](#)]
95. Ozga, A.J.; Chow, M.T.; Luster, A.D. Chemokines and the immune response to cancer. *Immunity* **2021**, *54*, 859–874. [[CrossRef](#)]
96. Hutchinson, L. Immunotherapy: Harmonizing the immune response with a cancer vaccine. *Nat. Rev. Clin. Oncol.* **2012**, *9*, 487. [[CrossRef](#)]
97. Meng, J.; Zhang, P.; Chen, Q.; Wang, Z.; Gu, Y.; Ma, J.; Li, W.; Yang, C.; Qiao, Y.; Hou, Y.; et al. Two-pronged intracellular co-delivery of antigen and adjuvant for synergistic cancer immunotherapy. *Adv. Mater.* **2022**, *34*, e2202168. [[CrossRef](#)]
98. Gavilan, H.; Avugadda, S.K.; Fernandez-Cabada, T.; Soni, N.; Cassani, M.; Mai, B.T.; Chantrell, R.; Pellegrino, T. Magnetic nanoparticles and clusters for magnetic hyperthermia: Optimizing their heat performance and developing combinatorial therapies to tackle cancer. *Chem. Soc. Rev.* **2021**, *50*, 11614–11667. [[CrossRef](#)]
99. Li, Y.; Chen, W.; Qi, Y.; Wang, S.; Li, L.; Li, W.; Xie, T.; Zhu, H.; Tang, Z.; Zhou, M. H₂S-Scavenged and activated iron oxide–hydroxide nanospindles for MRI–guided photothermal therapy and ferroptosis in lung cancer. *Small* **2020**, *16*, e2001356. [[CrossRef](#)]
100. Sun, X.; Liu, B.; Chen, X.; Lin, H.; Peng, Y.; Li, Y.; Zheng, H.; Xu, Y.; Ou, X.; Yan, S.; et al. Aptamer-assisted superparamagnetic iron oxide nanoparticles as multifunctional drug delivery platform for chemo-photodynamic combination therapy. *J. Mater. Sci. Mater. Med.* **2019**, *30*, 76. [[CrossRef](#)]
101. Yu, T.T.; Peng, X.C.; Wang, M.F.; Han, N.; Xu, H.Z.; Li, Q.R.; Li, L.G.; Xu, X.; Ma, Q.L.; Liu, B.; et al. Harnessing chlorin e6 loaded by functionalized iron oxide nanoparticles linked with glucose for target photodynamic therapy and improving of the immunogenicity of lung cancer. *J. Cancer Res. Clin. Oncol.* **2022**, *148*, 867–879. [[CrossRef](#)]
102. Wang, D.; Fei, B.; Halig, L.V.; Qin, X.; Hu, Z.; Xu, H.; Wang, Y.A.; Chen, Z.; Kim, S.; Shin, D.M.; et al. Targeted iron-oxide nanoparticle for photodynamic therapy and imaging of head and neck cancer. *ACS Nano* **2014**, *8*, 6620–6632. [[CrossRef](#)] [[PubMed](#)]
103. Huang, H.; Yuan, G.; Xu, Y.; Gao, Y.; Mao, Q.; Zhang, Y.; Bai, L.; Li, W.; Wu, A.; Hu, W.; et al. Photoacoustic and magnetic resonance imaging-based gene and photothermal therapy using mesoporous nanoagents. *Bioact. Mater.* **2022**, *9*, 157–167. [[CrossRef](#)] [[PubMed](#)]
104. Feng, Q.; Zhang, Y.; Zhang, W.; Hao, Y.; Wang, Y.; Zhang, H.; Hou, L.; Zhang, Z. Programmed near-infrared light-responsive drug delivery system for combined magnetic tumor-targeting magnetic resonance imaging and chemo-phototherapy. *Acta Biomater.* **2017**, *49*, 402–413. [[CrossRef](#)] [[PubMed](#)]
105. Khaledian, M.; Nourbakhsh, M.S.; Saber, R.; Hashemzadeh, H.; Darvishi, M.H. Preparation and evaluation of doxorubicin-loaded PLA-PEG-FA copolymer containing superparamagnetic iron oxide nanoparticles (SPIONs) for cancer treatment: Combination therapy with hyperthermia and chemotherapy. *Int. J. Nanomed.* **2020**, *15*, 6167–6182. [[CrossRef](#)]
106. Wang, K.; Tepper, J.E. Radiation therapy-associated toxicity: Etiology, management, and prevention. *CA Cancer J. Clin.* **2021**, *71*, 437–454. [[CrossRef](#)]
107. Ouyang, J.; Xie, A.; Zhou, J.; Liu, R.; Wang, L.; Liu, H.; Kong, N.; Tao, W. Minimally invasive nanomedicine: Nanotechnology in photo-/ultrasound-/radiation-/magnetism-mediated therapy and imaging. *Chem. Soc. Rev.* **2022**, *51*, 4996–5041. [[CrossRef](#)]
108. Anuje, M.; Pawaskar, P.N.; Khot, V.; Sivan, A.; Jadhav, S.; Meshram, J.; Thombare, B. Synthesis, Characterization, and cytotoxicity evaluation of polyethylene glycol–coated iron oxide nanoparticles for radiotherapy application. *J. Med. Phys.* **2021**, *46*, 154–161. [[CrossRef](#)]
109. Kievit, F.M.; Wang, K.; Ozawa, T.; Tarudji, A.W.; Silber, J.R.; Holland, E.C.; Ellenbogen, R.G.; Zhang, M. Nanoparticle-mediated knockdown of DNA repair sensitizes cells to radiotherapy and extends survival in a genetic mouse model of glioblastoma. *Nanomedicine* **2017**, *13*, 2131–2139. [[CrossRef](#)]
110. Kievit, F.M.; Stephen, Z.R.; Wang, K.; Dayringer, C.J.; Sham, J.G.; Ellenbogen, R.G.; Silber, J.R.; Zhang, M. Nanoparticle mediated silencing of DNA repair sensitizes pediatric brain tumor cells to gamma-irradiation. *Mol. Oncol.* **2015**, *9*, 1071–1080. [[CrossRef](#)]
111. Zhang, Y.; Wang, X.; Chu, C.; Zhou, Z.; Chen, B.; Pang, X.; Lin, G.; Lin, H.; Guo, Y.; Ren, E.; et al. Genetically engineered magnetic nanocages for cancer magneto-catalytic theranostics. *Nat. Commun.* **2020**, *11*, 5421. [[CrossRef](#)] [[PubMed](#)]
112. Jiang, S.; Eltoukhy, A.A.; Love, K.T.; Langer, R.; Anderson, D.G. Lipidoid-coated iron oxide nanoparticles for efficient DNA and siRNA delivery. *Nano Lett.* **2013**, *13*, 1059–1064. [[CrossRef](#)] [[PubMed](#)]
113. Hayashi, K.; Nakamura, M.; Miki, H.; Ozaki, S.; Abe, M.; Matsumoto, T.; Sakamoto, W.; Yogo, T.; Ishimura, K. Magnetically responsive smart nanoparticles for cancer treatment with a combination of magnetic hyperthermia and remote-control drug release. *Theranostics* **2014**, *4*, 834–844. [[CrossRef](#)]
114. Raguram, A.; Banskota, S.; Liu, D.R. Therapeutic in vivo delivery of gene editing agents. *Cell* **2022**, *185*, 2806–2827. [[CrossRef](#)] [[PubMed](#)]

115. Yin, H.; Kauffman, K.J.; Anderson, D.G. Delivery technologies for genome editing. *Nat. Rev. Drug Discov.* **2017**, *16*, 387–399. [[CrossRef](#)]
116. Mintzer, M.A.; Simanek, E.E. Nonviral vectors for gene delivery. *Chem. Rev.* **2009**, *109*, 259–302. [[CrossRef](#)]
117. Canton, I.; Battaglia, G. Endocytosis at the nanoscale. *Chem. Soc. Rev.* **2012**, *41*, 2718–2739. [[CrossRef](#)]
118. Hufschmid, R.; Teeman, E.; Mehdi, B.L.; Krishnan, K.M.; Browning, N.D. Observing the colloidal stability of iron oxide nanoparticles in situ. *Nanoscale* **2019**, *11*, 13098–13107. [[CrossRef](#)]
119. Saber Braim, F.; Noor Ashikin Nik Ab Razak, N.; Abdul Aziz, A.; Qasim Ismael, L.; Kayode Sodipo, B. Ultrasound assisted chitosan coated iron oxide nanoparticles: Influence of ultrasonic irradiation on the crystallinity, stability, toxicity and magnetization of the functionalized nanoparticles. *Ultrason. Sonochem.* **2022**, *88*, 106072. [[CrossRef](#)]
120. Min, K.A.; Cho, J.H.; Song, Y.K.; Kim, C.K. Iron casein succinylate-chitosan coacervate for the liquid oral delivery of iron with bioavailability and stability enhancement. *Arch. Pharm. Res.* **2016**, *39*, 94–102. [[CrossRef](#)]
121. Zhang, T.Y.; Li, F.Y.; Xu, Q.H.; Wang, Q.Y.; Jiang, X.C.; Liang, Z.Y.; Liao, H.W.; Kong, X.L.; Liu, J.A.; Wu, H.H.; et al. Ferrimagnetic nanochains-based mesenchymal stem cell engineering for highly efficient post-stroke recovery. *Adv. Funct. Mater.* **2019**, *29*, 1900603. [[CrossRef](#)]
122. Xu, Q.; Zhang, T.; Wang, Q.; Jiang, X.; Li, A.; Li, Y.; Huang, T.; Li, F.; Hu, Y.; Ling, D.; et al. Uniformly sized iron oxide nanoparticles for efficient gene delivery to mesenchymal stem cells. *Int. J. Pharm.* **2018**, *552*, 443–452. [[CrossRef](#)] [[PubMed](#)]
123. Mohammadi, M.R.; Malkovskiy, A.V.; Jothimuthu, P.; Kim, K.M.; Parekh, M.; Inayathullah, M.; Zhuge, Y.; Rajadas, J. PEG/Dextran double layer influences Fe ion release and colloidal stability of iron oxide nanoparticles. *Sci. Rep.* **2018**, *8*, 4286. [[CrossRef](#)] [[PubMed](#)]
124. Champagne, P.O.; Westwick, H.; Bouthillier, A.; Sawan, M. Colloidal stability of superparamagnetic iron oxide nanoparticles in the central nervous system: A review. *Nanomedicine* **2018**, *13*, 1385–1400. [[CrossRef](#)] [[PubMed](#)]
125. Mondini, S.; Drago, C.; Ferretti, A.M.; Puglisi, A.; Ponti, A. Colloidal stability of iron oxide nanocrystals coated with a PEG-based tetra-catechol surfactant. *Nanotechnology* **2013**, *24*, 105702. [[CrossRef](#)]
126. Park, Y.C.; Smith, J.B.; Pham, T.; Whitaker, R.D.; Sucato, C.A.; Hamilton, J.A.; Bartolak-Suki, E.; Wong, J.Y. Effect of PEG molecular weight on stability, T(2) contrast, cytotoxicity, and cellular uptake of superparamagnetic iron oxide nanoparticles (SPIONs). *Colloids Surf B Biointerfaces* **2014**, *119*, 106–114. [[CrossRef](#)]
127. Wheeler, K.E.; Chetwynd, A.J.; Fahy, K.M.; Hong, B.S.; Tochihuitl, J.A.; Foster, L.A.; Lynch, I. Environmental dimensions of the protein corona. *Nat. Nanotechnol.* **2021**, *16*, 617–629. [[CrossRef](#)]
128. Ren, J.; Andrikopoulos, N.; Velonia, K.; Tang, H.; Cai, R.; Ding, F.; Ke, P.C.; Chen, C. Chemical and biophysical signatures of the protein corona in nanomedicine. *J. Am. Chem. Soc.* **2022**, *144*, 9184–9205. [[CrossRef](#)]
129. Pustulka, S.M.; Ling, K.; Pish, S.L.; Champion, J.A. Protein nanoparticle charge and hydrophobicity govern protein corona and macrophage uptake. *ACS Appl. Mater. Interfaces* **2020**, *12*, 48284–48295. [[CrossRef](#)]
130. Bewersdorff, T.; Glitscher, E.A.; Bergueiro, J.; Eravci, M.; Miceli, E.; Haase, A.; Calderon, M. The influence of shape and charge on protein corona composition in common gold nanostructures. *Mater. Sci. Eng. C Mater. Biol. Appl.* **2020**, *117*, 111270. [[CrossRef](#)]
131. Chen, F.; Wang, G.; Griffin, J.I.; Brennehan, B.; Banda, N.K.; Holers, V.M.; Backos, D.S.; Wu, L.; Moghimi, S.M.; Simberg, D. Complement proteins bind to nanoparticle protein corona and undergo dynamic exchange in vivo. *Nat. Nanotechnol.* **2017**, *12*, 387–393. [[CrossRef](#)] [[PubMed](#)]
132. Tenzer, S.; Docter, D.; Kuharev, J.; Musyanovych, A.; Fetz, V.; Hecht, R.; Schlenk, F.; Fischer, D.; Kiouptsi, K.; Reinhardt, C.; et al. Rapid formation of plasma protein corona critically affects nanoparticle pathophysiology. *Nat. Nanotechnol.* **2013**, *8*, 772–781. [[CrossRef](#)] [[PubMed](#)]
133. Tengjisi; Hui, Y.; Fan, Y.; Zou, D.; Talbo, G.H.; Yang, G.; Zhao, C.X. Influence of nanoparticle mechanical property on protein corona formation. *J. Colloid Interface Sci.* **2022**, *606*, 1737–1744. [[CrossRef](#)] [[PubMed](#)]
134. Diaz-Diestra, D.M.; Palacios-Hernandez, T.; Liu, Y.; Smith, D.E.; Nguyen, A.K.; Todorov, T.; Gray, P.J.; Zheng, J.; Skoog, S.A.; Goering, P.L. Impact of surface chemistry of ultrasmall superparamagnetic iron oxide nanoparticles on protein corona formation and endothelial cell uptake, toxicity, and barrier function. *Toxicol. Sci.* **2022**, *188*, 261–275. [[CrossRef](#)]
135. Portilla, Y.; Mellid, S.; Paradela, A.; Ramos-Fernandez, A.; Daviu, N.; Sanz-Ortega, L.; Perez-Yague, S.; Morales, M.P.; Barber, D.F. Iron oxide nanoparticle coatings dictate cell outcomes despite the influence of protein coronas. *ACS Appl. Mater. Interfaces* **2021**, *13*, 7924–7944. [[CrossRef](#)]
136. Dobrovolskaia, M.A.; Aggarwal, P.; Hall, J.B.; McNeil, S.E. Preclinical studies to understand nanoparticle interaction with the immune system and its potential effects on nanoparticle biodistribution. *Mol. Pharm.* **2008**, *5*, 487–495. [[CrossRef](#)]
137. Rabel, M.; Warncke, P.; Thurmer, M.; Gruttner, C.; Bergemann, C.; Kurland, H.D.; Muller, F.A.; Koeberle, A.; Fischer, D. The differences of the impact of a lipid and protein corona on the colloidal stability, toxicity, and degradation behavior of iron oxide nanoparticles. *Nanoscale* **2021**, *13*, 9415–9435. [[CrossRef](#)]
138. Safi, M.; Courtois, J.; Seigneuret, M.; Conjeaud, H.; Berret, J.F. The effects of aggregation and protein corona on the cellular internalization of iron oxide nanoparticles. *Biomaterials* **2011**, *32*, 9353–9363. [[CrossRef](#)]
139. Groult, H.; Ruiz-Cabello, J.; Lechuga-Vieco, A.V.; Mateo, J.; Benito, M.; Bilbao, I.; Martinez-Alcazar, M.P.; Lopez, J.A.; Vazquez, J.; Herranz, F.F. Phosphatidylcholine-coated iron oxide nanomicelles for in vivo prolonged circulation time with an antibiofouling protein corona. *Chemistry* **2014**, *20*, 16662–16671. [[CrossRef](#)]

140. Ni, F.; Jiang, L.; Yang, R.; Chen, Z.; Qi, X.; Wang, J. Effects of PEG length and iron oxide nanoparticles size on reduced protein adsorption and non-specific uptake by macrophage cells. *J. Nanosci. Nanotechnol.* **2012**, *12*, 2094–2100. [[CrossRef](#)]
141. Revia, R.A.; Zhang, M. Magnetite nanoparticles for cancer diagnosis, treatment, and treatment monitoring: Recent advances. *Mater. Today* **2016**, *19*, 157–168. [[CrossRef](#)] [[PubMed](#)]
142. Wada, S.; Yue, L.; Tazawa, K.; Furuta, I.; Nagae, H.; Takemori, S.; Minamimura, T. New local hyperthermia using dextran magnetite complex (DM) for oral cavity: Experimental study in normal hamster tongue. *Oral Dis.* **2001**, *7*, 192–195. [[CrossRef](#)] [[PubMed](#)]
143. Schmitz, S.A.; Coupland, S.E.; Gust, R.; Winterhalter, S.; Wagner, S.; Kresse, M.; Semmler, W.; Wolf, K.J. Superparamagnetic iron oxide—enhanced MRI of atherosclerotic plaques in Watanabe hereditary hyperlipidemic rabbits. *Investig. Radiol.* **2000**, *35*, 460–471. [[CrossRef](#)]
144. Benjaminsen, R.V.; Matthebjerg, M.A.; Henriksen, J.R.; Moghimi, S.M.; Andresen, T.L. The possible “proton sponge” effect of polyethylenimine (PEI) does not include change in lysosomal pH. *Mol. Ther.* **2013**, *21*, 149–157. [[CrossRef](#)]
145. Skladanowski, A.; Bozko, P.; Sabisz, M. DNA structure and integrity checkpoints during the cell cycle and their role in drug targeting and sensitivity of tumor cells to anticancer treatment. *Chem. Rev.* **2009**, *109*, 2951–2973. [[CrossRef](#)]
146. Duan, X.; Li, Y. Physicochemical characteristics of nanoparticles affect circulation, biodistribution, cellular internalization, and trafficking. *Small* **2013**, *9*, 1521–1532. [[CrossRef](#)] [[PubMed](#)]
147. Ling, D.; Lee, N.; Hyeon, T. Chemical synthesis and assembly of uniformly sized iron oxide nanoparticles for medical applications. *Acc. Chem. Res.* **2015**, *48*, 1276–1285. [[CrossRef](#)] [[PubMed](#)]
148. Larsen, E.K.; Nielsen, T.; Wittenborn, T.; Birkedal, H.; Vorup—Jensen, T.; Jakobsen, M.H.; Ostergaard, L.; Horsman, M.R.; Besenbacher, F.; Howard, K.A.; et al. Size-dependent accumulation of PEGylated silane—coated magnetic iron oxide nanoparticles in murine tumors. *ACS Nano* **2009**, *3*, 1947–1951. [[CrossRef](#)]
149. Laurent, S.; Saei, A.A.; Behzadi, S.; Panahifar, A.; Mahmoudi, M. Superparamagnetic iron oxide nanoparticles for delivery of therapeutic agents: Opportunities and challenges. *Expert Opin. Drug Deliv.* **2014**, *11*, 1449–1470. [[CrossRef](#)]
150. Hu, Y.; Mignani, S.; Majoral, J.P.; Shen, M.; Shi, X. Construction of iron oxide nanoparticle—based hybrid platforms for tumor imaging and therapy. *Chem. Soc. Rev.* **2018**, *47*, 1874–1900. [[CrossRef](#)]
151. Tong, S.; Quinto, C.A.; Zhang, L.; Mohindra, P.; Bao, G. Size-dependent heating of magnetic iron oxide nanoparticles. *ACS Nano* **2017**, *11*, 6808–6816. [[CrossRef](#)] [[PubMed](#)]
152. Boselli, L.; Polo, E.; Castagnola, V.; Dawson, K.A. Regimes of biomolecular ultrasmall nanoparticle interactions. *Angew. Chem. Int. Ed. Engl.* **2017**, *56*, 4215–4218. [[CrossRef](#)]
153. Park, J.H.; von Maltzahn, G.; Zhang, L.; Derfus, A.M.; Simberg, D.; Harris, T.J.; Ruoslahti, E.; Bhatia, S.N.; Sailor, M.J. Systematic surface engineering of magnetic nanoworms for in vivo tumor targeting. *Small.* **2009**, *5*, 694–700. [[CrossRef](#)]
154. Roca, A.G.; Gutierrez, L.; Gavilan, H.; Fortes Brollo, M.E.; Veintemillas-Verdaguer, S.; Morales, M.D.P. Design strategies for shape—controlled magnetic iron oxide nanoparticles. *Adv. Drug Deliv. Rev.* **2019**, *138*, 68–104. [[CrossRef](#)]
155. Groult, H.; Garcia-Alvarez, I.; Romero-Ramirez, L.; Nieto-Sampedro, M.; Herranz, F.; Fernandez-Mayoralas, A.; Ruiz-Cabello, J. Micellar iron oxide nanoparticles coated with anti-tumor glycosides. *Nanomaterials* **2018**, *8*, 567. [[CrossRef](#)]
156. Truong, N.P.; Whittaker, M.R.; Mak, C.W.; Davis, T.P. The importance of nanoparticle shape in cancer drug delivery. *Expert Opin. Drug Deliv.* **2015**, *12*, 129–142. [[CrossRef](#)]
157. Park, J.H.; von Maltzahn, G.; Zhang, L.; Schwartz, M.P.; Ruoslahti, E.; Bhatia, S.N.; Sailor, M.J. Magnetic iron oxide nanoworms for tumor targeting and imaging. *Adv. Mater.* **2008**, *20*, 1630–1635. [[CrossRef](#)] [[PubMed](#)]
158. Chauhan, V.P.; Popovic, Z.; Chen, O.; Cui, J.; Fukumura, D.; Bawendi, M.G.; Jain, R.K. Fluorescent nanorods and nanospheres for real—time in vivo probing of nanoparticle shape—dependent tumor penetration. *Angew. Chem. Int. Ed. Engl.* **2011**, *50*, 11417–11420. [[CrossRef](#)] [[PubMed](#)]
159. Kinnear, C.; Moore, T.L.; Rodriguez-Lorenzo, L.; Rothen-Rutishauser, B.; Petri-Fink, A. Form follows function: Nanoparticle shape and its implications for nanomedicine. *Chem. Rev.* **2017**, *117*, 11476–11521. [[CrossRef](#)]
160. Liu, Z.; Cai, W.; He, L.; Nakayama, N.; Chen, K.; Sun, X.; Chen, X.; Dai, H. In vivo biodistribution and highly efficient tumour targeting of carbon nanotubes in mice. *Nat. Nanotechnol.* **2007**, *2*, 47–52. [[CrossRef](#)] [[PubMed](#)]
161. Geng, Y.; Dalhaimer, P.; Cai, S.; Tsai, R.; Tewari, M.; Minko, T.; Discher, D.E. Shape effects of filaments versus spherical particles in flow and drug delivery. *Nat. Nanotechnol.* **2007**, *2*, 249–255. [[CrossRef](#)]
162. Vyas, D.; Patel, M.; Wairkar, S. Strategies for active tumor targeting—An update. *Eur. J. Pharm.* **2022**, *915*, 174512. [[CrossRef](#)] [[PubMed](#)]
163. Park, D.H.; Cho, J.; Kwon, O.J.; Yun, C.O.; Choy, J.H. Biodegradable inorganic nanovector: Passive versus active tumor targeting in siRNA transportation. *Angew. Chem. Int. Ed. Engl.* **2016**, *55*, 4582–4586. [[CrossRef](#)] [[PubMed](#)]
164. Zhang, Y.; Cao, J.; Yuan, Z. Strategies and challenges to improve the performance of tumor-associated active targeting. *J. Mater. Chem. B* **2020**, *8*, 3959–3971. [[CrossRef](#)] [[PubMed](#)]
165. Xu, Y.; Wu, H.; Huang, J.; Qian, W.; Martinson, D.E.; Ji, B.; Li, Y.; Wang, Y.A.; Yang, L.; Mao, H. Probing and enhancing ligand-mediated active targeting of tumors using Sub-5 nm ultrafine iron oxide nanoparticles. *Theranostics* **2020**, *10*, 2479–2494. [[CrossRef](#)]
166. Upadhyay, A.; Kandi, R.; Rao, C.P. Wheat germ agglutinin modified magnetic iron oxide nanocomplex as a cell membrane specific receptor target material for killing breast cancer cells. *J. Mater. Chem. B* **2018**, *6*, 5729–5737. [[CrossRef](#)]

167. Zhang, J.; Chen, N.; Wang, H.; Gu, W.; Liu, K.; Ai, P.; Yan, C.; Ye, L. Dual-targeting superparamagnetic iron oxide nanoprobe with high and low target density for brain glioma imaging. *J. Colloid. Interface Sci.* **2016**, *469*, 86–92. [[CrossRef](#)] [[PubMed](#)]
168. Chen, L.; Wu, Y.; Wu, H.; Li, J.; Xie, J.; Zang, F.; Ma, M.; Gu, N.; Zhang, Y. Magnetic targeting combined with active targeting of dual-ligand iron oxide nanoprobe to promote the penetration depth in tumors for effective magnetic resonance imaging and hyperthermia. *Acta Biomater.* **2019**, *96*, 491–504. [[CrossRef](#)]
169. Wang, Z.; Qiao, R.; Tang, N.; Lu, Z.; Wang, H.; Zhang, Z.; Xue, X.; Huang, Z.; Zhang, S.; Zhang, G.; et al. Active targeting theranostic iron oxide nanoparticles for MRI and magnetic resonance-guided focused ultrasound ablation of lung cancer. *Biomaterials* **2017**, *127*, 25–35. [[CrossRef](#)] [[PubMed](#)]
170. Chen, K.; Xie, J.; Xu, H.; Behera, D.; Michalski, M.H.; Biswal, S.; Wang, A.; Chen, X. Triblock copolymer coated iron oxide nanoparticle conjugate for tumor integrin targeting. *Biomaterials* **2009**, *30*, 6912–6919. [[CrossRef](#)] [[PubMed](#)]
171. Ebadi, M.; Bullo, S.; Buskaran, K.; Hussein, M.Z.; Fakurazi, S.; Pastorin, G. Dual-functional iron oxide nanoparticles coated with polyvinyl alcohol/5-fluorouracil/zinc-aluminium-layered double hydroxide for a simultaneous drug and target delivery system. *Polymers* **2021**, *13*, 855. [[CrossRef](#)]
172. Hu, Q.; Li, H.; Wang, L.; Gu, H.; Fan, C. DNA Nanotechnology-enabled drug delivery systems. *Chem. Rev.* **2019**, *119*, 6459–6506. [[CrossRef](#)] [[PubMed](#)]
173. Tan, M.; Xu, Y.; Gao, Z.; Yuan, T.; Liu, Q.; Yang, R.; Zhang, B.; Peng, L. Recent Advances in intelligent wearable medical devices integrating biosensing and drug delivery. *Adv. Mater.* **2022**, *34*, e2108491. [[CrossRef](#)] [[PubMed](#)]
174. Torchilin, V.P. Multifunctional, stimuli-sensitive nanoparticulate systems for drug delivery. *Nat. Rev. Drug Discov.* **2014**, *13*, 813–827. [[CrossRef](#)] [[PubMed](#)]
175. Singh, N.; Son, S.; An, J.; Kim, I.; Choi, M.; Kong, N.; Tao, W.; Kim, J.S. Nanoscale porous organic polymers for drug delivery and advanced cancer theranostics. *Chem. Soc. Rev.* **2021**, *50*, 12883–12896. [[CrossRef](#)]
176. Feng, L.; Dong, Z.; Tao, D.; Zhang, Y.; Liu, Z. The acidic tumor microenvironment: A target for smart cancer nano-theranostics. *Natl. Sci. Rev.* **2018**, *5*, 269–286. [[CrossRef](#)]
177. Liu, M.; Huang, L.; Zhang, W.; Wang, X.; Geng, Y.; Zhang, Y.; Wang, L.; Zhang, W.; Zhang, Y.J.; Xiao, S.; et al. A transistor-like pH-sensitive nanodetergent for selective cancer therapy. *Nat. Nanotechnol.* **2022**, *17*, 541–551. [[CrossRef](#)] [[PubMed](#)]
178. Cao, Y.; Huang, H.Y.; Chen, L.Q.; Du, H.H.; Cui, J.H.; Zhang, L.W.; Lee, B.J.; Cao, Q.R. Enhanced lysosomal escape of pH-responsive polyethylenimine-betaine functionalized carbon nanotube for the codelivery of survivin small interfering RNA and Doxorubicin. *ACS Appl. Mater. Interfaces* **2019**, *11*, 9763–9776. [[CrossRef](#)]
179. Wang, Z.; Liu, G.; Zheng, H.; Chen, X. Rigid nanoparticle-based delivery of anti-cancer siRNA: Challenges and opportunities. *Biotechnol. Adv.* **2014**, *32*, 831–843. [[CrossRef](#)] [[PubMed](#)]
180. Kwon, Y.J. Before and after endosomal escape: Roles of stimuli-converting siRNA/polymer interactions in determining gene silencing efficiency. *Acc. Chem. Res.* **2012**, *45*, 1077–1088. [[CrossRef](#)]
181. Shim, M.S.; Kwon, Y.J. Acid-responsive linear polyethylenimine for efficient, specific, and biocompatible siRNA delivery. *Bioconjug. Chem.* **2009**, *20*, 488–499. [[CrossRef](#)]
182. Zhao, Z.; Li, M.; Zeng, J.; Huo, L.; Liu, K.; Wei, R.; Ni, K.; Gao, J. Recent advances in engineering iron oxide nanoparticles for effective magnetic resonance imaging. *Bioact. Mater.* **2022**, *12*, 214–245. [[CrossRef](#)]
183. Zhang, T.; Lin, R.; Wu, H.; Jiang, X.; Gao, J. Mesenchymal stem cells: A living carrier for active tumor-targeted delivery. *Adv. Drug Deliv. Rev.* **2022**, *185*, 114300. [[CrossRef](#)]